Available online at www.sciencedirect.com
ScienceDirect
International Journal of Solids and Structures 44 (2007) 8119–8142
INTERNATIONAL JOURNAL OF SOLIDS AND STRUCTURES
www.elsevier.com/locate/ijsolstr

Interlaminar hygrothermal stresses in laminated plates

Arash Bahrami, Asghar Nosier *

Department of Mechanical Engineering, Sharif University of Technology, P.O. Box 11365-9567, Azadi Avenue, Tehran, Iran

Received 17 March 2007; received in revised form 31 May 2007
Available online 10 June 2007

Abstract

Within the elasticity formulation the most general displacement field for hygrothermal problems of long laminated composite plates is presented. The equivalent single-layer theories are then employed to determine the global deformation parameters appearing in the displacement fields of general cross-ply, symmetric, and antisymmetric angle-ply laminates under thermal and hygroscopic loadings. Reddy's layerwise theory is subsequently used to determine the local deformation parameters of various displacement fields. An elasticity solution is also developed in order to validate the efficiency and accuracy of the layerwise theory in predicting the interlaminar normal and shear stress distributions. Finally, various numerical results are presented for edge-effect problems of several cross-ply, symmetric, and antisymmetric angle-ply laminates subjected to uniform hygrothermal loads. All results indicate high stress gradients of interlaminar normal and shear stresses near the edges of laminates.

Keywords: Laminated plates; Interlaminar stresses; Elasticity formulation; Equivalent single-layer theories; Layerwise theory; Hygrothermal loading

1. Introduction

With the ever-increasing applications of laminated composites in severe environmental conditions hygrothermal behavior of such laminates has attracted considerable attention. The interlaminar normal and shear stresses, on the other hand, are believed to play a significant role in prediction of dominant cause of failure in composite laminates. These stresses that exhibit highly localized concentration near the edges of the laminate are the basis for damage in the form of free-edge delamination and the subsequent delamination growth in the interior region of laminates, leading to failure at loads below those corresponding to in plane failure. Therefore among the extensive research areas in the analysis of fiber-reinforced composites, the issue of interlaminar-edge stresses has been subject of tremendous investigations and various theoretical and experimental methods are employed to study the edge-effect problem of composite laminates. Since, the present study is devoted to thermal and hygroscopic problems, in the proceeding only the pertinent works will be referred. A relatively comprehensive review of the various techniques of evaluation of interlaminar stresses that have

* Corresponding author. Tel.: +98 21 6616 5543; fax: +98 21 6600 0021.
E-mail address: nosier@sharif.edu (A. Nosier).

0020-7683/$ - see front matter © 2007 Elsevier Ltd. All rights reserved.
doi:10.1016/j.ijsolstr.2007.06.004

appeared in the literature is available in the survey paper by Kant and Swaminathan (2000). Examination of the literature survey reveals that the first paper considering the thermal loading in the edge-effect problem of composite laminates is developed by Pagano (1974). He utilized a higher-order shear deformation theory (HSDT) to formulate the edge-effect problem of symmetric balanced laminates subjected to a constant axial strain and a constant temperature change. Based on the formulation presented by Pipes and Pagano (1970), Wang and Crossman (1977a,b) studied the free-edge stresses in symmetric balanced laminates under a uniform thermal load using a finite element procedure. An approximate elasticity solution was presented by Wang and Choi (1982) to determine the boundary-layer stresses due to hygroscopic effects. Wang and Chou (1989) obtained the transient interlaminar thermal stresses in symmetric balanced laminate by means of a zeroth-order perturbation analysis of the equilibrium equations. Webber and Morton (1993) and Morton and Webber (1993) by following a similar approach to that used by Kassapoglou and Lagace (1986, 1987), attempted to calculate the interlaminar free-edge stress distribution in symmetric laminates subjected to thermal loads. By employing the complementary energy approach together with polynomial expansion of stress functions, Yin (1997) proposed a variational method to evaluate the thermal interlaminar stresses. Also Kim and Atlury (1995) developed an stress-based variational method to obtain interlaminar stresses under combined thermo-mechanical loading. In an effort to determine the interlaminar stresses, an iterative technique in conjunction with the extended Kantorovich method is presented by Cho and Kim (2000) for thermal and mechanical loads. Rohwer et al. (2001) investigated the transverse shear and normal stresses in composite laminates subjected to thermal loading by using the extended two-dimensional method and the first-order shear deformation plate theory (FSDT). A two-dimensional global higher-order deformation theory was proposed by Matsunaga (2004) for the calculation of out-of-plane stresses in cross-ply laminates subjected to thermal loading. Recently, a comprehensive examination of interlaminar stresses in general cross-ply laminates has been presented by Tahani and Nosier (2003, 2004). They used a layerwise theory to predict free-edge stresses in finite general cross-ply laminates under various mechanical, thermal, and hygroscopic loadings.

Despite the intensive investigations on the analysis of interlaminar stresses in composite laminates, documented in the literature during the past three decades, few publications focused on the study of such stresses under hygrothermal loading conditions. In addition, for the case of hygrothermal loading, reliable numerical results are limited to cross-ply and symmetric balanced laminates. The purpose of the present work, however, is to analyze the interlaminar stresses in symmetric and unsymmetric cross-ply laminates, symmetric laminates, and antisymmetric angle-ply laminates subjected to uniform thermal and/or hygroscopic loadings. Towards this goal, both equivalent single-layer (ESL) and layerwise theories (LWT) are utilized. Each of the ESL and layerwise models has its advantages and disadvantages in terms of solution accuracy, solution economy, and simplicity. The ESL models which follow from an assumed global displacement field lead to the definition of effective overall rigidities and are incapable of providing precise calculation of local 3-D stress field. On the other hand, the layerwise models which possess the ability of accurately describing the three-dimensional effects, such as free-edge stresses, are computationally expensive. Thus, it is attempted here to introduce a solution scheme which achieves maximum solution accuracy with minimal solution cost by employing an efficient analytical procedure. This, on the other hand, is done by utilizing an appropriate ESL theory to determine the unknown constant parameters appearing in various laminates displacement fields. Interlaminar stresses are then determined by using an analysis based on the layerwise theory of Reddy. Lastly, an analytical elasticity solution is presented for a specific set of boundary and loading conditions in order to assess the effectiveness and validity of the present developments.

2. Theoretical formulation

The laminate considered in the present investigation is of thickness h, width $2b$, and assumed to be long in the x-direction so that the strain components are functions of y and z only (Fig. 1). It is further assumed that the mechanical loads (if present) are applied at $x = -a$ and $x = a$ only. Also the thermal and hygrothermal loadings are considered to be uniform everywhere in the laminate. Under these conditions the most general form of the displacement field within the kth layer of the laminate has been shown to be as follows (Nosier and Bahrami, 2007; Lekhnitskii, 1981):

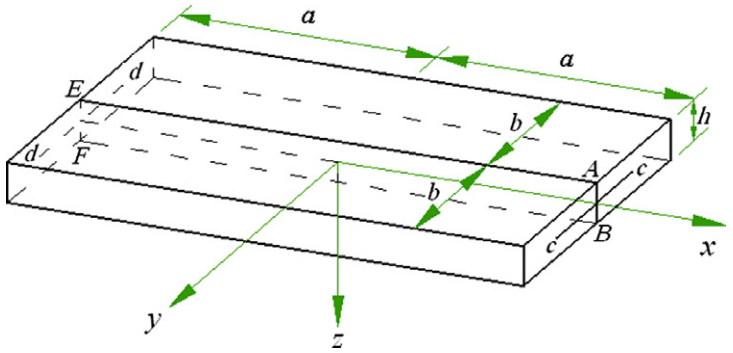

Fig. 1. Laminate geometry and coordinate system.

$$\begin{aligned} u_1^{(k)}(x,y,z) &= B_4xy + B_6xz + B_2x + u^{(k)}(y,z) \\ u_2^{(k)}(x,y,z) &= -B_1xz + B_3x - \frac{1}{2}B_4x^2 + v^{(k)}(y,z) \\ u_3^{(k)}(x,y,z) &= B_1xy + B_5x - \frac{1}{2}B_6x^2 + w^{(k)}(y,z) \end{aligned} \tag{1}$$

where, $u_1^{(k)}(x,y,z)$, $u_2^{(k)}(x,y,z)$, and $u_3^{(k)}(x,y,z)$ represent the displacement components in the x-, y-, and z-directions, respectively, of a material point initially located at (x,y,z) in the kth lamina of the laminate. It is next noted that as long as the loading conditions at $x=-a$ and $x=a$ are similar (so that the laminate in Fig. 1 is globally in equilibrium), the following conditions will hold:

$$\begin{aligned} u_1^{(k)}(x,y,z) &= -u_1^{(k)}(-x,-y,z) \\ u_2^{(k)}(x,y,z) &= -u_2^{(k)}(-x,-y,z) \\ u_3^{(k)}(x,y,z) &= u_3^{(k)}(-x,-y,z). \end{aligned} \tag{2}$$

Upon imposing these restrictions on (1) it is readily seen that the constants B_4 and B_5 must vanish and the displacement field in (1) is, therefore, reduced to what follows:

$$u_1^{(k)}(x,y,z) = B_2x + B_6xz + u^{(k)}(y,z) \tag{3a}$$

$$u_2^{(k)}(x,y,z) = -B_1xz + B_3x + v^{(k)}(y,z) \tag{3b}$$

$$u_3^{(k)}(x,y,z) = B_1xy - \tfrac{1}{2}B_6x^2 + w^{(k)}(y,z). \tag{3c}$$

Furthermore, by replacing $u^{(k)}(y,z)$ appearing in (3a) by $-B_3\,y + u^{(k)}(y,z)$, it becomes apparent that the terms involving B_3 in (3) will generate no strains and, therefore, can be omitted (these terms, in fact, will correspond to an infinitesimal rotation of the laminate about the z-axis in Fig. 1). Thus, the most general form of an arbitrary laminated composite laminate is given as follows:

$$u_1^{(k)}(x,y,z) = B_2x + B_6xz + u^{(k)}(y,z) \tag{4a}$$

$$u_2^{(k)}(x,y,z) = -B_1xz + v^{(k)}(y,z) \tag{4b}$$

$$u_3^{(k)}(x,y,z) = B_1xy - \tfrac{1}{2}B_6x^2 + w^{(k)}(y,z). \tag{4c}$$

The displacement field in (4) may be used, in principle, for calculating the stress field in any composite laminate subjected to arbitrary combinations of self-equilibrating mechanical and uniform hygrothermal loads. In the present study, however, our attention is focused on symmetric and unsymmetric cross-ply laminates, symmetric laminates, and antisymmetric angle-ply laminates subjected to uniform hygroscopic and thermal

loadings. Since the solutions developed here in the present study significantly depend on the lamination scheme, each of the aforementioned laminates is examined separately.

2.1. Cross-ply laminates

For symmetric and unsymmetric cross-ply laminates (e.g., see Jones, 1998) subjected to uniform hygrothermal loadings, based on physical grounds, the following restrictions will, furthermore, hold (see Fig. 1):

$$u_1^{(k)}(x,y,z) = -u_1^{(k)}(-x,y,z) \tag{5a}$$

$$u_2^{(k)}(x,y,z) = u_2^{(k)}(-x,y,z). \tag{5b}$$

Upon imposing (5a) on (4a) it is concluded that $u^{(k)}(y,z) = 0$. Also from (5b) and (4b) it is concluded that $B_1 = 0$. Thus, for cross-ply laminates the most general form of the displacement field is given as follows:

$$\begin{aligned} u_1^{(k)}(x,y,z) &= B_2 x + B_6 xz \\ u_2^{(k)}(x,y,z) &= v^{(k)}(y,z) \\ u_3^{(k)}(x,y,z) &= -\frac{1}{2}B_6 x^2 + w^{(k)}(y,z). \end{aligned} \tag{6}$$

It is to be noted that for symmetric cross-ply laminates it can readily be shown that (see Eqs. (8) below) $B_6 = 0$.

2.2. Symmetric laminates

For symmetrically laminated composite plates (e.g., see Jones, 1998) under uniform hygrothermal loadings the deformational behavior of the material points within the laminates remains the same with respect to the middle surface. Thus, the following restrictions must hold with respect to the middle surface of any symmetric laminate with N layers:

$$u_1^{(k)}(x,y,z) = u_1^{(N-k+1)}(x,y,-z) \tag{7a}$$

$$u_2^{(k)}(x,y,z) = u_2^{(N-k+1)}(x,y,-z). \tag{7b}$$

From (7a) and (4a), it is concluded that $B_6 = 0$. Also from (7b) and (4b) it is concluded that $B_1 = 0$. Therefore, for symmetric laminates the most general form of the displacement field is given as:

$$\begin{aligned} u_1^{(k)}(x,y,z) &= B_2 x + u^{(k)}(y,z) \\ u_2^{(k)}(x,y,z) &= v^{(k)}(y,z) \\ u_3^{(k)}(x,y,z) &= w^{(k)}(y,z). \end{aligned} \tag{8}$$

2.3. Antisymmetric angle-ply laminates

For antisymmetric angle-ply laminates with N layers (e.g., see Jones, 1998) subjected to uniform hygrothermal loadings the following condition must hold (see also Nosier and Bahrami, 2007):

$$u_1^{(k)}(x,y,z) = u_1^{(N-k+1)}(x,-y,-z). \tag{9}$$

From (9) and (4a) it is concluded that $B_6 = 0$ and, therefore, the most general displacement field for such laminates is given as follows:

$$\begin{aligned} u_1^{(k)}(x,y,z) &= B_2 x + u^{(k)}(y,z) \\ u_2^{(k)}(x,y,z) &= -B_1 xz + v^{(k)}(y,z) \\ u_3^{(k)}(x,y,z) &= B_1 xy + w^{(k)}(y,z). \end{aligned} \tag{10}$$

The displacement fields in (6), (8), and (10) can be represented in one place as:

$$
\begin{aligned}
u_1^{(k)}(x,y,z) &= B_2 x + \delta_C B_6 xz + \delta_{AS} u^{(k)}(y,z) \\
u_2^{(k)}(x,y,z) &= -\delta_A B_1 xz + v^{(k)}(y,z) \\
u_3^{(k)}(x,y,z) &= \delta_A B_1 xy - \frac{1}{2}\delta_C B_6 x^2 + w^{(k)}(y,z)
\end{aligned} \tag{11}
$$

where $\delta_A = \delta_{AS} = 0$ and $\delta_C = 1$ for unsymmetric cross-ply laminates, $\delta_A = \delta_C = 0$ and $\delta_{AS} = 1$ for symmetric laminates, and $\delta_A = \delta_{AS} = 1$ and $\delta_C = 0$ for antisymmetric angle-ply laminates. It is to be noted that the terms involving the constant parameters B_1, B_2, and B_6 describe the global deformations within the laminates whereas the functions $u^{(k)}(y,z)$, $v^{(k)}(y,z)$, and $w^{(k)}(y,z)$ correspond to the local deformations of kth layer within the laminate.

2.4. Equivalent single-layer theories

It is well known by now that ESL theories are adequate in predicting the global responses of the composite laminates. On the other hand, these theories are simpler and computationally less time consuming than the layerwise theories. The objective of the present section is to present the simplest ESL theory which, on the other hand, will provide sufficiently accurate results for the unknown constant parameters B_1, B_2, and B_6 appearing in (11). For unsymmetric cross-ply and antisymmetric angle-ply laminates numerical studies conducted by the authors indicate the first-order shear deformation theory of plates (FSDT), also known as Mindlin–Reissner plate theory, is fairly accurate in predicting these parameters. For symmetric laminates, however, an improved first-order theory must be developed and used for determining the appropriate constant parameter (i.e., B_2) appearing in the displacement field (11).

In FSDT the components of the displacement vector at a material point in the laminate are expressed in the following form (Reddy, 2003):

$$
\begin{aligned}
u_1(x,y,z) &= u(x,y) + z\psi_x(x,y) \\
u_2(x,y,z) &= v(x,y) + z\psi_y(x,y) \\
u_3(x,y,z) &= w(x,y)
\end{aligned} \tag{12}
$$

where u, v, and w denote the displacements of a point located on the middle plane of the laminate. Also ψ_x and ψ_y are the rotations of transverse normals about the y- and x-axes, respectively. The displacement field in (6) indicates that for hygrothermal problems of cross-ply laminates the displacement field within FSDT (i.e., Eq. (12)) must take the following simpler form:

$$
\begin{aligned}
u_1(x,y,z) &= B_2 x + B_6 xz \\
u_2(x,y,z) &= V(y) + z\Psi_y(y) \\
u_3(x,y,z) &= -\tfrac{1}{2}B_6 x^2 + W(y)
\end{aligned} \tag{13}
$$

with B_6 being equal to zero when the cross-ply laminate is symmetric. Similarly, based on the displacement field in (10), it is concluded that for hygrothermal problems of antisymmetric angle-ply laminates the displacement field within FSDT must take the following simpler form:

$$
\begin{aligned}
u_1(x,y,z) &= B_2 x + U(y) + z\Psi_x(y) \\
u_2(x,y,z) &= -B_1 xz + V(y) + z\Psi_y(y) \\
u_3(x,y,z) &= B_1 xy + W(y).
\end{aligned} \tag{14}
$$

As it is pointed out earlier, for symmetric laminates FSDT is incapable of accurately determining the unknown parameter B_2 appearing in (8). This is attributed to the fact that, when such laminates are subjected to uniform hygrothermal loads, the unknown functions ψ_x, ψ_y, and w vanish and the remaining terms in (12) will not be adequate for accurate determination of B_2. On the other hand, in symmetric laminates under hygrothermal loadings the displacement components u_1, u_2 must be even functions of thickness coordinate z whereas u_3 must be an odd function of z. For such laminates it is found that a more accurate result for B_2 may be found by introducing the following displacement field:

$$\begin{aligned} u_1(x,y,z) &= u(x,y) + |z|\tilde{\psi}_x(x,y) \\ u_2(x,y,z) &= v(x,y) + |z|\tilde{\psi}_y(x,y) \\ u_3(x,y,z) &= z\psi_z(x,y). \end{aligned} \tag{15}$$

Numerical studies reveal, furthermore, that the thickness stretching term (i.e., $z\psi_z$) introduced in (15) has a negligible effect on the accuracy of B_2 and, therefore, can be omitted when symmetric laminates are subjected to uniform hygrothermal loadings. Based on the displacement field in (8), it is, thus, concluded that the simplest appropriate displacement field for symmetric laminates is given as follows:

$$\begin{aligned} u_1(x,y,z) &= B_2 x + U(y) + |z|\tilde{\Psi}_x(y) \\ u_2(x,y,z) &= V(y) + |z|\tilde{\Psi}_y(y) \\ u_3(x,y,z) &= 0. \end{aligned} \tag{16}$$

The theory that will be developed here using (16) will be referred to as the improved first-order shear deformation plate theory (IFSDT). It remains to find and, thereafter, solve the equilibrium equations corresponding to the displacement fields in Eqs. (13), (14), and (16) in order to determine the constant parameters existing in these displacement fields. For brevity, however, here the detail of the procedure is demonstrated for the displacement field in (16) only and the results corresponding to the displacement fields in (13) and (14) are summarized. By using the displacement field (16) in the principle of minimum total potential energy (Fung and Tong, 2001) and treating the constant B_2 as an unknown parameter five equilibrium equations are obtained which may be presented as follows:

$$\delta U : N'_{xy} = 0 \tag{17a}$$

$$\delta V : N'_{y} = 0 \tag{17b}$$

$$\delta\tilde{\Psi}_x : \tilde{Q}_x - \tilde{M}'_{xy} = 0 \tag{17c}$$

$$\delta\tilde{\Psi}_y : \tilde{Q}_y - \tilde{M}'_{y} = 0 \tag{17d}$$

$$\delta B_2 : \int_{-b}^{b} N_x \,\mathrm{d}y = 0 \tag{18}$$

where a prime indicates an ordinary differentiation with respect to variable y and the stress and moment resultants appearing in (17) and (18) are defined as follows:

$$\begin{aligned} &(N_x, N_y, N_{xy}) = \int_{-h/2}^{h/2} (\sigma_x, \sigma_y, \sigma_{xy})\,\mathrm{d}z, \quad (\tilde{Q}_x, \tilde{Q}_y) = \int_{-h/2}^{h/2} \mathrm{sgn}(z)(\sigma_{xz}, \sigma_{yz})\,\mathrm{d}z \\ &(\tilde{M}_y, \tilde{M}_{xy}) = \int_{-h/2}^{h/2} |z|(\sigma_y, \sigma_{xy})\,\mathrm{d}z \end{aligned} \tag{19a}$$

with

$$\mathrm{sgn}(z) = \begin{cases} -1 & \text{for } z < 0 \\ 1 & \text{for } z > 0. \end{cases} \tag{19b}$$

Upon substitution of the displacement field (16) into Eq. (19a), through the linear strain-displacement relations of elasticity and the plane-stress constitutive law (Herakovich, 1998) of a lamina, the stress and moment resultants may be expressed as:

$$\begin{Bmatrix} N_x \\ N_y \\ N_{xy} \\ \tilde{M}_y \\ \tilde{M}_{xy} \end{Bmatrix} = \begin{bmatrix} A_{16} & A_{12} & \tilde{B}_{16} & \tilde{B}_{12} & A_{11} \\ A_{26} & A_{22} & \tilde{B}_{26} & \tilde{B}_{22} & A_{12} \\ A_{66} & A_{26} & \tilde{B}_{66} & \tilde{B}_{26} & A_{16} \\ \tilde{B}_{26} & \tilde{B}_{22} & D_{26} & D_{22} & \tilde{B}_{12} \\ \tilde{B}_{66} & \tilde{B}_{26} & D_{66} & D_{26} & \tilde{B}_{16} \end{bmatrix} \begin{Bmatrix} U' \\ V' \\ \tilde{\Psi}'_x \\ \tilde{\Psi}'_y \\ B_2 \end{Bmatrix} - \begin{Bmatrix} N_x^{\mathrm{T}} \\ N_y^{\mathrm{T}} \\ N_{xy}^{\mathrm{T}} \\ \tilde{M}_y^{\mathrm{T}} \\ \tilde{M}_{xy}^{\mathrm{T}} \end{Bmatrix} - \begin{Bmatrix} N_x^{\mathrm{H}} \\ N_y^{\mathrm{H}} \\ N_{xy}^{\mathrm{H}} \\ \tilde{M}_y^{\mathrm{H}} \\ \tilde{M}_{xy}^{\mathrm{H}} \end{Bmatrix} \tag{20a}$$

and

$$\begin{Bmatrix} \tilde{Q}_y \\ \tilde{Q}_x \end{Bmatrix} = k^2 \begin{bmatrix} A_{44} & A_{45} \\ A_{45} & A_{55} \end{bmatrix} \begin{Bmatrix} \tilde{\Psi}_y \\ \tilde{\Psi}_x \end{Bmatrix} \tag{20b}$$

where the laminate rigidities A_{ij}, $\tilde{B}_{ij}$, and D_{ij} are defined as:

$$(A_{ij}, \tilde{B}_{ij}, D_{ij}) = \int_{-h/2}^{h/2} \bar{Q}_{ij}(1, |z|, z^2)\,\mathrm{d}z \tag{21}$$

with $\bar{Q}_{ij}$ being the transformed reduced stiffness (Herakovich, 1998) of an orthotropic lamina. Also N^{T}, $\tilde{M}^{\mathrm{T}}$ are referred to as the thermal resultants and defined as:

$$(N_x^{\mathrm{T}}, N_y^{\mathrm{T}}, N_{xy}^{\mathrm{T}}) = \int_{-h/2}^{h/2} \left[(\bar{Q}_{11}, \bar{Q}_{12}, \bar{Q}_{16})\alpha_x + (\bar{Q}_{12}, \bar{Q}_{22}, \bar{Q}_{26})\alpha_y + (\bar{Q}_{16}, \bar{Q}_{26}, \bar{Q}_{66})\alpha_{xy}\right] \Delta T\ \mathrm{d}z \tag{22a}$$

$$(\tilde{M}_y^{\mathrm{T}}, \tilde{M}_{xy}^{\mathrm{T}}) = \int_{-h/2}^{h/2} \left[(\bar{Q}_{12}, \bar{Q}_{16})\alpha_x + (\bar{Q}_{22}, \bar{Q}_{26})\alpha_y + (\bar{Q}_{26}, \bar{Q}_{66})\alpha_{xy}\right] \Delta T|z|\,\mathrm{d}z \tag{22b}$$

where ΔT denotes the temperature change and α_x, α_y, and α_{xy} denote the transformed coefficients of thermal expansions (Herakovich, 1998). The hygroscopic resultants are, similarly, defined as:

$$(N_x^{\mathrm{H}}, N_y^{\mathrm{H}}, N_{xy}^{\mathrm{H}}) = \int_{-h/2}^{h/2} \left[(\bar{Q}_{11}, \bar{Q}_{12}, \bar{Q}_{16})\beta_x + (\bar{Q}_{12}, \bar{Q}_{22}, \bar{Q}_{26})\beta_y + (\bar{Q}_{16}, \bar{Q}_{26}, \bar{Q}_{66})\beta_{xy}\right] \Delta M\ \mathrm{d}z \tag{23a}$$

$$(\tilde{M}_y^{\mathrm{H}}, \tilde{M}_{xy}^{\mathrm{H}}) = \int_{-h/2}^{h/2} \left[(\bar{Q}_{12}, \bar{Q}_{16})\beta_x + (\bar{Q}_{22}, \bar{Q}_{26})\beta_y + (\bar{Q}_{26}, \bar{Q}_{66})\beta_{xy}\right] \Delta M|z|\,\mathrm{d}z. \tag{23b}$$

In Eqs. (23), ΔM is the percent moisture (by weight) absorbed by each layer in the laminate and β_x, β_y, and β_{xy} indicate the transformed coefficients of hygroscopic expansions (Herakovich, 1998). Also in (20b) the constant k^2 is called the shear correction factor which is often introduced for in a first-order theory to modify the laminate transverse shear rigidities.

For free edges of the laminate at $y = \pm b$ according to the principle of minimum total potential energy the following traction-free boundary conditions must be imposed:

$$N_y = N_{xy} = 0 \quad \text{at } y = \pm b \tag{24a}$$

and

$$\tilde{M}_{xy} = \tilde{M}_y = 0 \quad \text{at } y = \pm b. \tag{24b}$$

Integrating the equilibrium equations in (17a) and (17b) and imposing the boundary conditions in (24a) yield:

$$N_y(y) = N_{xy}(y) = 0. \tag{25}$$

These conditions are used to express U' and V' appearing in (20a) in terms of $\tilde{\Psi}_x$ and $\tilde{\Psi}_y$, and B_2. This way the resultants N_x, $\tilde{M}_y$, and $\tilde{M}_{xy}$ are all expressed in terms of $\tilde{\Psi}_x$ and $\tilde{\Psi}_y$, and B_2. Finally, upon substitution of $\tilde{M}_{xy}$ and $\tilde{M}_y$, and (20b) into the equilibrium equations (17c) and (17d), the following results are obtained:

$$\delta\tilde{\Psi}_x : \bar{D}_{66}\tilde{\Psi}''_x - k^2 A_{55}\tilde{\Psi}_x + \bar{D}_{26}\tilde{\Psi}''_y - k^2 A_{45}\tilde{\Psi}_y = 0 \tag{26a}$$

$$\delta\tilde{\Psi}_y : \bar{D}_{26}\tilde{\Psi}''_x - k^2 A_{45}\tilde{\Psi}_x + \bar{D}_{22}\tilde{\Psi}''_y - k^2 A_{44}\tilde{\Psi}_y = 0 \tag{26b}$$

with the coefficients $\bar{D}_{22}$, $\bar{D}_{26}$, and $\bar{D}_{66}$ being displayed in Appendix A. Upon imposing the boundary conditions in (24b) on the general solution of (26), the generalized displacement functions $\tilde{\Psi}_x$ and $\tilde{\Psi}_y$ are obtained in terms of the unknown constant B_2 which, on the other hand, may be presented as follows:

$$\tilde{\Psi}_x(y) = \sum_{j=1}^{2} A_j \sinh(\lambda_j y), \quad \tilde{\Psi}_y(y) = \sum_{j=1}^{2} \bar{D}_j A_j \sinh(\lambda_j y) \tag{27}$$

where the coefficients A_j and $\bar{D}_j$ $(j = 1, 2)$ are given as:

$$A_1 = d_1 B_2 + m_y^{\mathrm{T}} + m_y^{\mathrm{H}} \tag{28a}$$

$$A_2 = d_2 B_2 + m_{xy}^{\mathrm{T}} + m_{xy}^{\mathrm{H}} \tag{28b}$$

$$\bar{D}_j = -\frac{\bar{D}_{66}\lambda_j^2 - k^2 A_{55}}{\bar{D}_{26}\lambda_j^2 - k^2 A_{45}} \ (j = 1, 2). \tag{28c}$$

The constant parameters appearing in (28a) and (28b) are presented in Appendix A. In addition, λ_j^2 $(j = 1, 2)$ appearing in (28c) are the roots of the following characteristic equation (associated with Eqs. (26)):

$$(\lambda^2 \bar{D}_{66} - k^2 A_{55})(\lambda^2 \bar{D}_{22} - k^2 A_{44}) - (\lambda^2 \bar{D}_{26} - k^2 A_{45})^2 = 0. \tag{29}$$

Finally, upon substituting (27) into the stress resultant N_x and the subsequent result into the global equilibrium equation (18), the constant parameter B_2 is determined which, on the other hand, may be presented as follows:

$$B_2 = \frac{1}{\hat{h}}(n_x^{\mathrm{T}} + n_x^{\mathrm{H}}) \tag{30}$$

where the expressions for $\hat{h}$, n_x^{T}, and n_x^{H} are also listed in Appendix A.

It is remarked earlier that a procedure similar to that outlined here for symmetric laminates may be employed to determine the unknown parameters appearing in the displacement fields of unsymmetric cross-ply and antisymmetric angle-ply laminates. For brevity, however, only the appropriate results are presented here. For cross-ply laminates the constants B_2 and B_6 appearing in (13) are found to be as follows:

$$B_2 = \frac{1}{h_1 h_4 - h_2 h_3}\left[h_4\left(n_x^{\mathrm{T}} + n_x^{\mathrm{H}}\right) - h_2\left(m_x^{\mathrm{T}} + m_x^{\mathrm{H}}\right)\right] \tag{31a}$$

$$B_6 = \frac{1}{h_1 h_4 - h_2 h_3}\left[h_1\left(m_x^{\mathrm{T}} + m_x^{\mathrm{H}}\right) - h_3\left(n_x^{\mathrm{T}} + n_x^{\mathrm{H}}\right)\right]. \tag{31b}$$

The expressions for the constant parameters appearing in (31) are for clarity displayed in Appendix B. For antisymmetric angle-ply laminates the constants parameters B_1 and B_2 appearing in the displacement field (14) are found to be as follows:

$$B_1 = \frac{1}{h_1 h_4 - h_2 h_3}\left[h_4\left(n_x^{\mathrm{T}} + n_x^{\mathrm{H}}\right) - h_2\left(m_{xy}^{\mathrm{T}} + m_{xy}^{\mathrm{H}}\right)\right] \tag{32a}$$

$$B_2 = \frac{1}{h_1 h_4 - h_2 h_3}\left[h_1\left(m_{xy}^{\mathrm{T}} + m_{xy}^{\mathrm{H}}\right) - h_3\left(n_x^{\mathrm{T}} + n_x^{\mathrm{H}}\right)\right]. \tag{32b}$$

The constant parameters in (32) are listed in Appendix C.

2.5. Layerwise laminated plate theory of Reddy

Due to existence of local high stress gradient and the three-dimensional nature of the boundary-layer phenomenon, the interlaminar stresses in the boundary-layer regions can not be computed accurately by the ESL theories. Thus, Reddy's layerwise theory that is capable of modeling localized three-dimensional effects is utilized here to carry out the hygrothermal interlaminar stress analysis in laminates with free edges. The theory assumes that the displacement components of a generic point in the laminate are given by (Nosier et al., 1993):

$$\begin{aligned} u_1(x,y,z) &= u_k(x,y)\Phi_k(z) \\ u_2(x,y,z) &= v_k(x,y)\Phi_k(z) \quad k = 1,2,\ldots,N+1 \\ u_3(x,y,z) &= w_k(x,y)\Phi_k(z) \end{aligned} \tag{33}$$

with k being a dummy index indicating summation from 1 to $N+1$. In (33) u_1, u_2, and u_3 denote the displacement components in the x-, y-, and z-directions, respectively, of a material point located at (x,y,z) in the undeformed state. Also, $u_k(x,y)$, $v_k(x,y)$, and $w_k(x,y)$ indicate the displacements of all points located, initially, on the kth plane in the x-, y-, and z-directions, respectively. In addition, N corresponds to the total number of numerical layers considered in a laminate. Furthermore, $\Phi_k(z)$ are the global Lagrangian interpolation polynomials associated with the kth surface (see Tahani and Nosier, 2004; Reddy, 2003; Nosier et al., 1993). It is to be noted that the layerwise concept introduced here is very general in a sense that the accuracy of the solution can be improved as close as desired by increasing the number of the subdivisions through the thickness or increasing the order of interpolation polynomials through the thickness. However, in the present study, the interpolation functions $\Phi_k(z)$ are assumed to have linear variation through the thickness of each numerical layer. The elasticity-based displacement field in (11) indicates that the displacement field of LWT appearing in (33) must be rewritten in a simpler form as follows:

$$\begin{aligned} u_1(x,y,z) &= B_2 x + \delta_C B_6 xz + \delta_{AS} U_k(y)\Phi_k(z) \\ u_2(x,y,z) &= -\delta_A B_1 xz + V_k(y)\Phi_k(z) \qquad k = 1,2,\ldots,N+1 \\ u_3(x,y,z) &= \delta_A B_1 xy - \tfrac{1}{2}\delta_C B_6 x^2 + W_k(y)\Phi_k(z). \end{aligned} \tag{34}$$

Substitution of (34) into the linear strain–displacement relations of elasticity (e.g., see Fung and Tong, 2001) yields the following results:

$$\begin{aligned} &\varepsilon_x = B_2 + \delta_C B_6 z, \quad \varepsilon_y = V_k'\Phi_k, \quad \varepsilon_z = W_k\Phi_k', \quad \gamma_{yz} = W_k'\Phi_k + V_k\Phi_k' \\ &\gamma_{xz} = \delta_{AS} U_k\Phi_k' + \delta_A B_1 y, \quad \gamma_{xy} = \delta_{AS} U_k'\Phi_k - \delta_A B_1 z. \end{aligned} \tag{35}$$

The equilibrium equations of a laminate within LWT are obtained employing (35) in the principle of minimum potential energy (e.g., see Fung and Tong, 2001). The results are, in general, $3(N+1)$ local equilibrium equations corresponding to $3(N+1)$ unknown functions U_k, V_k, and W_k, and three global equations corresponding to the three unknown constants B_1, B_2, and B_6 as follows:

$$\delta U_k : \delta_{AS}\left(Q_x^k - \frac{dM_{xy}^k}{dy}\right) = 0 \tag{36a}$$

$$\delta V_k : Q_y^k - \frac{dM_y^k}{dy} = 0 \tag{36b}$$

$$\delta W_k : N_z^k - \frac{dR_y^k}{dy} = 0 \tag{36c}$$

$$\delta B_1 : \delta_A \int_{-h/2}^{h/2}\int_{-b}^{b} (\sigma_{xz} y - \sigma_{xy} z)\, dy\, dz = 0 \tag{37a}$$

$$\delta B_2 : \int_{-h/2}^{h/2}\int_{-b}^{b} \sigma_x\, dy\, dz = 0 \tag{37b}$$

$$\delta B_6 : \delta_C \int_{-h/2}^{h/2}\int_{-b}^{b} \sigma_x z\, dy\, dz = 0. \tag{37c}$$

Here, the generalized stress resultants, appearing in Eqs. (36a) through (36c), are defined as:

$$(M_y^k, M_{xy}^k, N_z^k) = \int_{-h/2}^{h/2} (\sigma_y \Phi_k, \sigma_{xy}\Phi_k, \sigma_z \Phi_k')\,\mathrm{d}z$$
$$(Q_x^k, Q_y^k, R_y^k) = \int_{-h/2}^{h/2} (\sigma_{xz}\Phi_k', \sigma_{yz}\Phi_k', \sigma_{yz}\Phi_k)\,\mathrm{d}z. \tag{38}$$

It is next noted that the three-dimensional stress–strain relations within the kth layer of composite laminate are given as (e.g., see Herakovich, 1998):

$$\{\sigma\}^{(k)} = [\bar{C}]^{(k)}\left(\{\varepsilon\} - \{\varepsilon^{\mathrm{T}}\} - \{\varepsilon^{\mathrm{H}}\}\right)^{(k)} \tag{39}$$

with $[\bar{C}]$ being the transformed stiffness matrix and $\{\varepsilon^{\mathrm{T}}\}$ and $\{\varepsilon^{\mathrm{H}}\}$ being the thermal and hygroscopic strains, respectively. By merely substituting relations (35) into (39) and the subsequent results into (38), the generalized stress resultants are expressed in terms of the displacement functions:

$$\begin{aligned}(M_y^k, M_{xy}^k, N_z^k) &= \delta_{\mathrm{AS}}(D_{26}^{kj}, D_{66}^{kj}, B_{36}^{jk})U_j' + (D_{22}^{kj}, D_{26}^{kj}, B_{23}^{jk})V_j' + (B_{23}^{kj}, B_{36}^{kj}, A_{33}^{kj})W_j \\ &\quad + (B_{12}^k, B_{16}^k, A_{13}^k)B_2 - \delta_{\mathrm{A}}(D_{26}^k, D_{66}^k, \bar{B}_{36}^k)B_1 + \delta_{\mathrm{C}}(D_{12}^k, D_{16}^k, \bar{B}_{13}^k)B_6 \\ &\quad - (M_y^{k(\mathrm{T})}, M_{xy}^{k(\mathrm{T})}, N_z^{k(\mathrm{T})}) - (M_y^{k(\mathrm{H})}, M_{xy}^{k(\mathrm{H})}, N_z^{k(\mathrm{H})}) \\ (Q_x^k, Q_y^k, R_y^k) &= \delta_{\mathrm{AS}}(A_{55}^{kj}, A_{45}^{kj}, B_{45}^{kj})U_j + (A_{45}^{kj}, A_{44}^{kj}, B_{44}^{kj})V_j + (B_{45}^{jk}, B_{44}^{jk}, D_{44}^{kj})W_j' \\ &\quad + \delta_{\mathrm{A}}(A_{55}^k, A_{45}^k, B_{45}^k)B_1 y\end{aligned} \tag{40}$$

where the expressions for laminate rigidities and the thermal and hygroscopic resultants are listed in Appendix D. Lastly, upon substitution of Eqs. (40) into (36) and (37), the governing equations of equilibrium are obtained in the following form:

$$\delta U_k : \delta_{\mathrm{AS}}\left[D_{66}^{kj}U_j'' - A_{55}^{kj}U_j + D_{26}^{kj}V_j'' - A_{45}^{kj}V_j + (B_{36}^{kj} - B_{45}^{jk})W_j'\right] = \delta_{\mathrm{A}}B_1 A_{55}^k y \tag{41a}$$

$$\delta V_k : \delta_{\mathrm{AS}}D_{26}^{kj}U_j'' - \delta_{\mathrm{AS}}A_{45}^{kj}U_j + D_{22}^{kj}V_j'' - A_{44}^{kj}V_j + (B_{23}^{kj} - B_{44}^{jk})W_j' = \delta_{\mathrm{A}}B_1 A_{45}^k y \tag{41b}$$

$$\begin{aligned}\delta W_k &: \delta_{\mathrm{AS}}(B_{45}^{kj} - B_{36}^{jk})U_j' + (B_{44}^{kj} - B_{23}^{jk})V_j' + D_{44}^{kj}W_j'' - A_{33}^{kj}W_j \\ &= B_2 A_{13}^k - \delta_{\mathrm{A}}B_1(B_{45}^k + \bar{B}_{36}^k) + \delta_{\mathrm{C}}\bar{B}_{13}^k B_6 - N_z^{k(\mathrm{T})} - N_z^{k(\mathrm{H})}\end{aligned} \tag{41c}$$

$$\begin{aligned}\delta B_1 &: \delta_{\mathrm{A}}\int_{-b}^{b}\Big[(\delta_{\mathrm{AS}}A_{55}^j U_j + A_{45}^j V_j + B_{45}^j W_j')y - (\delta_{\mathrm{AS}}D_{66}^j U_j' + D_{26}^j V_j' + \bar{B}_{36}^j W_j) \\ &\quad + \delta_{\mathrm{A}}B_1(A_{55}y^2 + D_{66}) - B_2 B_{16} - \delta_{\mathrm{C}}B_6 D_{16} + M_{xy}^T + M_{xy}^H\Big]\,\mathrm{d}y = 0\end{aligned} \tag{42a}$$

$$\delta B_2 : \int_{-b}^{b}\left[\delta_{\mathrm{AS}}B_{16}^j U_j' + B_{12}^j V_j' + A_{13}^j W_j + B_2 A_{11} + \delta_{\mathrm{C}}B_6 B_{11} - \delta_{\mathrm{A}}B_1 B_{16} - N_x^T - N_x^H\right]\mathrm{d}y = 0 \tag{42b}$$

$$\delta B_6 : \delta_{\mathrm{C}}\int_{-b}^{b}\left[\delta_{\mathrm{AS}}D_{16}^j U_j' + D_{12}^j V_j' + \bar{B}_{13}^j W_j + B_2 B_{11} + \delta_{\mathrm{C}}B_6 D_{11} - \delta_{\mathrm{A}}B_1 D_{16} - M_x^T - M_x^H\right]\mathrm{d}y = 0. \tag{42c}$$

To investigate the free-edge-effect problem, Eqs. (41) and (42) must be solved subject to the following traction-free boundary conditions at $y = \pm b$:

$$\delta_{\mathrm{AS}}M_{xy}^k = M_y^k = R_y^k = 0 \quad \text{at } y = \pm b. \tag{43}$$

As it is seen from (41) the local displacement equations comprise of $3(N+1)$ coupled second-order differential equations with constant coefficients. It is clear that such a linear system may be solved analytically using, for example, the state space approach. This way, the displacement components will be found, in general, in terms of B_1, B_2, B_6, and $6(N+1)$ constants of integration. Three global displacement equations in (42) and $6(N+1)$ boundary conditions in (43) are, then, employed to determine integration constants and unknown coefficients B_1, B_2, and B_6. A detailed description of the solution scheme has been presented in Nosier and Bahrami (2006, 2007) and, therefore, for brevity will not be repeated here. It is to be noted that the constant parameters B_1, B_2, and B_6 appearing in (34) may be considered to be known from an analysis based on the first-order theories

developed here (see Eqs. (30) through (32)) since they represent global response quantities of laminates. In fact the accuracy of the first-order theories in predicting these parameters will be assessed within the present study when numerical results are discussed.

2.6. Theory of elasticity

In order to verify the validity of the solutions obtained in the previous sections, an analytical elasticity solution is presented here for particular boundary and loading conditions. A generally stacked laminate subjected to a uniform hygrothermal loading is considered. It is, moreover, assumed that the ends of the laminate in Fig. 1 are gripped so that the line AB (EF) is not allowed to have rotations about the x-axis and the line cc (the x-axis and the line dd). Under such assumptions the constants B_1 and B_6 vanish and the displacement field of elasticity in (4) is simplified to what follows:

$$\begin{aligned} u_1^{(k)}(x,y,z) &= B_2 x + u^{(k)}(y,z) \\ u_2^{(k)}(x,y,z) &= v^{(k)}(y,z) \\ u_3^{(k)}(x,y,z) &= w^{(k)}(y,z). \end{aligned} \tag{44}$$

The constant B_2 appearing in (44) represents the uniform axial strain in the x-direction due to a hygrothermal loading and will be determined here within the elasticity theory. By employing the displacement field (44) in the principle of minimum total potential energy (e.g., see Fung and Tong, 2001) the local and global equilibrium equations are readily found to be:

$$\delta u : \frac{\partial \sigma_{xy}^{(k)}}{\partial y} + \frac{\partial \sigma_{xz}^{(k)}}{\partial z} = 0 \tag{45a}$$

$$\delta v : \frac{\partial \sigma_{y}^{(k)}}{\partial y} + \frac{\partial \sigma_{yz}^{(k)}}{\partial z} = 0 \tag{45b}$$

$$\delta w : \frac{\partial \sigma_{yz}^{(k)}}{\partial y} + \frac{\partial \sigma_{z}^{(k)}}{\partial z} = 0 \tag{45c}$$

and

$$\delta B_2 : \int_{-b}^{b} \int_{-h/2}^{h/2} \sigma_x \, \mathrm{d}z \, \mathrm{d}y = 0, \tag{46}$$

respectively. For traction-free boundary conditions at $y = \pm b$, no analytical solution seems to exist for Eqs. (45a) through (45c). It is, however, noted that Eqs. (45) admit an analytical solution for the following boundary conditions at $y = \pm b$:

$$\sigma_y^{(k)} = u_3^{(k)} = \sigma_{xy}^{(k)} = 0 \quad \text{at } y = \pm b. \tag{47}$$

Using the three-dimensional stress–strain relations in (39) together with strain-displacement relationships of elasticity (e.g., see Fung and Tong, 2001), the local equilibrium equations in (45) may be expressed in terms of the displacement components as follows:

$$\begin{aligned} &\bar{C}_{66}^{(k)} u_{,yy}^{(k)} + \bar{C}_{55}^{(k)} u_{,zz}^{(k)} + \bar{C}_{26}^{(k)} v_{,yy}^{(k)} + \bar{C}_{45}^{(k)} v_{,zz}^{(k)} + (\bar{C}_{45}^{(k)} + \bar{C}_{36}^{(k)}) w_{,yz}^{(k)} = 0 \\ &\bar{C}_{26}^{(k)} u_{,yy}^{(k)} + \bar{C}_{45}^{(k)} u_{,zz}^{(k)} + \bar{C}_{22}^{(k)} v_{,yy}^{(k)} + \bar{C}_{44}^{(k)} v_{,zz}^{(k)} + (\bar{C}_{23}^{(k)} + \bar{C}_{44}^{(k)}) w_{,yz}^{(k)} = 0 \\ &(\bar{C}_{45}^{(k)} + \bar{C}_{36}^{(k)}) u_{,yz}^{(k)} + (\bar{C}_{23}^{(k)} + \bar{C}_{44}^{(k)}) v_{,yz}^{(k)} + \bar{C}_{44}^{(k)} w_{,yy}^{(k)} + \bar{C}_{33}^{(k)} w_{,zz}^{(k)} = 0 \end{aligned} \tag{48}$$

where a coma followed by a variable denotes partial differentiation with respect to that variable. Similarly, the boundary conditions in (47) are expressed in terms of the displacement components as follows:

$$
\begin{aligned}
&\bar{C}_{26}^{(k)}u_{,y}^{(k)} + \bar{C}_{22}^{(k)}v_{,y}^{(k)} + \bar{C}_{23}^{(k)}w_{,z}^{(k)} = \bar{C}_{12}^{(k)}(\varepsilon_x^{k(\mathrm{T})} + \varepsilon_x^{k(\mathrm{H})} - B_2) \\
&\quad + \bar{C}_{22}^{(k)}(\varepsilon_y^{k(\mathrm{T})} + \varepsilon_y^{k(\mathrm{H})}) + \bar{C}_{23}^{(k)}(\varepsilon_z^{k(\mathrm{T})} + \varepsilon_z^{k(\mathrm{H})}) + \bar{C}_{26}^{(k)}(\gamma_{xy}^{k(\mathrm{T})} + \gamma_{xy}^{k(\mathrm{H})}) \\
&\bar{C}_{66}^{(k)}u_{,y}^{(k)} + \bar{C}_{26}^{(k)}v_{,y}^{(k)} + \bar{C}_{36}^{(k)}w_{,z}^{(k)} = \bar{C}_{16}^{(k)}(\varepsilon_x^{k(\mathrm{T})} + \varepsilon_x^{k(\mathrm{H})} - B_2) \quad \text{at } y = \pm b \\
&\quad + \bar{C}_{26}^{(k)}(\varepsilon_y^{k(\mathrm{T})} + \varepsilon_y^{k(\mathrm{H})}) + \bar{C}_{36}^{(k)}(\varepsilon_z^{k(\mathrm{T})} + \varepsilon_z^{k(\mathrm{H})}) + \bar{C}_{66}^{(k)}(\gamma_{xy}^{k(\mathrm{T})} + \gamma_{xy}^{k(\mathrm{H})}) \\
&w^{(k)} = 0.
\end{aligned}
\tag{49}
$$

It remains next to obtain the solution of Eqs. (48) satisfying the boundary conditions in (49) and the following conditions:

The traction-free conditions at the top surface of the first layer:

$$\sigma_z^{(1)} = \sigma_{yz}^{(1)} = \sigma_{xz}^{(1)} = 0 \text{ at the top surface of the 1st layer.} \tag{50a}$$

The traction-free conditions at the bottom surface of the Nth layer:

$$\sigma_z^{(N)} = \sigma_{yz}^{(N)} = \sigma_{xz}^{(N)} = 0 \text{ at the bottom surface of the } N\text{th layer.} \tag{50b}$$

The displacement continuity conditions at every interface within the laminate:

$$u_1^{(k)} = u_1^{(k+1)}, u_2^{(k)} = u_2^{(k+1)}, \text{ and } u_3^{(k)} = u_3^{(k+1)} \text{ at interfaces.} \tag{50c}$$

The stress equilibrium conditions at every interface within the laminate:

$$\sigma_z^{(k)} = \sigma_z^{(k+1)}, \sigma_{yz}^{(k)} = \sigma_{yz}^{(k+1)}, \text{ and } \sigma_{xz}^{(k)} = \sigma_{xz}^{(k+1)} \text{ at interfaces.} \tag{50d}$$

Eqs. (48) with the boundary conditions in (49) may be solved by means of the Fourier series technique. A complete description of the solution procedure is discussed in Nosier and Bahrami (2007) and, for the sake of brevity, is not repeated here. The displacement components within the kth layer of the laminate are found to be:

$$
\begin{aligned}
u_1^{(k)}(x,y,z) &= B_2 x + \sum_{m=0}^{\infty}\sum_{i=1}^{6} A_{kmi}\mathrm{e}^{\lambda_{kmi}z}\sin(\alpha_m y) + \sum_{m=1}^{\infty} A_{km}\sin(\alpha_m y) \\
u_2^{(k)}(x,y,z) &= \sum_{m=0}^{\infty}\sum_{i=1}^{6} \bar{B}_{kmi}A_{kmi}\mathrm{e}^{\lambda_{kmi}z}\sin(\alpha_m y) + \sum_{m=1}^{\infty} B_{km}\sin(\alpha_m y) \\
u_3^{(k)}(x,y,z) &= \sum_{m=0}^{\infty}\sum_{i=1}^{6} \bar{C}_{kmi}A_{kmi}\mathrm{e}^{\lambda_{kmi}z}\cos(\alpha_m y)
\end{aligned}
\tag{51}
$$

where $\alpha_m = (2m+1)\pi/2b$ and λ_{kmi} $(i = 1, 2, \ldots, 6)$ are the roots of the following sixth-order polynomial equation:

$$
\begin{vmatrix}
-\alpha_m^2\bar{C}_{66}^{(k)} + \bar{C}_{55}^{(k)}\lambda_{km}^2 & -\alpha_m^2\bar{C}_{26}^{(k)} + \lambda_{km}^2\bar{C}_{45}^{(k)} & -\alpha_m\lambda_{km}(\bar{C}_{45}^{(k)} + \bar{C}_{36}^{(k)}) \\
-\alpha_m^2\bar{C}_{26}^{(k)} + \bar{C}_{45}^{(k)}\lambda_{km}^2 & -\alpha_m^2\bar{C}_{22}^{(k)} + \lambda_{km}^2\bar{C}_{44}^{(k)} & -\alpha_m\lambda_{km}(\bar{C}_{44}^{(k)} + \bar{C}_{23}^{(k)}) \\
\alpha_m\lambda_{km}(\bar{C}_{45}^{(k)} + \bar{C}_{36}^{(k)}) & \alpha_m\lambda_{km}(\bar{C}_{44}^{(k)} + \bar{C}_{23}^{(k)}) & -\alpha_m^2\bar{C}_{44}^{(k)} + \lambda_{km}^2\bar{C}_{33}^{(k)}
\end{vmatrix} = 0.
\tag{52}
$$

Also the parameters A_{km} and B_{km} appearing in (51) are given by:

$$A_{km} = \frac{\bar{C}_{12}^{(k)}\bar{C}_{26}^{(k)} - \bar{C}_{16}^{(k)}\bar{C}_{22}^{(k)}}{\bar{C}_{66}^{(k)}\bar{C}_{22}^{(k)} - \bar{C}_{26}^{(k)^2}}B_2 a_m \quad \text{and} \quad B_{km} = \frac{\bar{C}_{16}^{(k)}\bar{C}_{26}^{(k)} - \bar{C}_{12}^{(k)}\bar{C}_{66}^{(k)}}{\bar{C}_{66}^{(k)}\bar{C}_{22}^{(k)} - \bar{C}_{26}^{(k)^2}}B_2 a_m \tag{53a}$$

with

$$a_m = \frac{8b}{\pi^2}\frac{(-1)^m}{(2m+1)^2}. \tag{53b}$$

Moreover, the coefficients $\bar{B}_{kmi}$ and $\bar{C}_{kmi}$ appearing in (51) are determined from the following relations:

$$\begin{Bmatrix} \bar{B}_{kmi} \\ \bar{C}_{kmi} \end{Bmatrix} = \begin{bmatrix} -\alpha_m^2 \bar{C}_{26}^{(k)} + \lambda_{kmi}^2 \bar{C}_{45}^{(k)} & -\alpha_m \lambda_{kmi} (\bar{C}_{45}^{(k)} + \bar{C}_{36}^{(k)}) \\ -\alpha_m^2 \bar{C}_{22}^{(k)} + \lambda_{kmi}^2 \bar{C}_{44}^{(k)} & -\alpha_m \lambda_{kmi} (\bar{C}_{44}^{(k)} + \bar{C}_{23}^{(k)}) \end{bmatrix}^{-1} \begin{Bmatrix} \alpha_m^2 \bar{C}_{66}^{(k)} - \bar{C}_{55}^{(k)} \lambda_{kmi}^2 \\ \alpha_m^2 \bar{C}_{26}^{(k)} - \bar{C}_{45}^{(k)} \lambda_{kmi}^2 \end{Bmatrix}. \tag{54}$$

The next step of the analysis is to determine the $6N$ unknowns, namely, A_{kmi} ($k = 1,2,\ldots,N$ and $i = 1,\ldots,6$) for each Fourier integer m and the unknown parameter B_2. These unknowns will be determined in a try and error process by imposing the conditions in (50a) through (50d) and Eq. (46). For this purpose, an initial value is assumed for B_2. This value is then substituted into conditions (50a) through (50d) to obtain a system of $6N$ algebraic equations in terms of A_{kmi} (for each m) which upon solving yields the unknown coefficients A_{kmi} ($k = 1,2,\ldots,N$ and $i = 1,\ldots,6$). Next, upon carrying out the integration in (46) a new B_2 is found which, on the other hand, may be presented as:

$$B_2 = \frac{1}{b\sum_{k=1}^{N} \bar{C}_{11}^{(k)} h_k} \left[\begin{array}{l} b(N_x^{\mathrm{T}} + N_x^{\mathrm{H}}) - \sum_{k=1}^{N} \sum_{m=1}^{\infty} h_k (\bar{C}_{12}^{(k)} B_{km} + \bar{C}_{16}^{(k)} A_{km})(-1)^m \\ -2 \sum_{k=1}^{N} \sum_{m=0}^{\infty} \sum_{i=1}^{6} \left(\frac{\bar{B}_{kmi} \bar{C}_{12}^{(k)} + \bar{C}_{16}^{(k)}}{\lambda_{kmi}} + \frac{\bar{C}_{kmi} \bar{C}_{13}^{(k)}}{\alpha_m} \right) A_{kmi} (-1)^m \sinh\left(\frac{\lambda_{kmi} h_k}{2}\right) \end{array} \right] \tag{55}$$

where N_x^{T} and N_x^{H} appearing in (55) are defined as:

$$\begin{aligned} N_x^{\mathrm{T}} &= \sum_{k=1}^{N} (\bar{C}_{11}^{(k)} \alpha_x^{(k)} + \bar{C}_{12}^{(k)} \alpha_y^{(k)} + \bar{C}_{13}^{(k)} \alpha_z^{(k)} + \bar{C}_{16}^{(k)} \alpha_{xy}^{(k)}) h_k \Delta T \\ N_x^{\mathrm{H}} &= \sum_{k=1}^{N} (\bar{C}_{11}^{(k)} \beta_x^{(k)} + \bar{C}_{12}^{(k)} \beta_y^{(k)} + \bar{C}_{13}^{(k)} \beta_z^{(k)} + \bar{C}_{16}^{(k)} \beta_{xy}^{(k)}) h_k \Delta M. \end{aligned} \tag{56}$$

It is reminded here that for convenience the z coordinate is located at the middle surface of each ply. The new value of B_2 is then compared with that assumed initially. If the difference between two values is significant, the new value of B_2 in (55) is used as the initial value and the procedure is repeated until B_2 is obtained with any desirable degree of accuracy. It is to be noted that by substituting B_2 into (53a) and subsequent results into (51) the displacement components will be obtained. Upon substitution of the displacement field into strain-displacement relations of linear elasticity (e.g., see Fung and Tong, 2001) and using the three-dimensional Hooke law (39) the stress components are finally determined.

It is pointed out that the elasticity solution presented here is, although analytical, not an exact solution since the Gibbs phenomenon appears in the Fourier expansions introduced in the solution procedure (see Nosier and Bahrami, 2007). In fact, according to the solution obtained here, the interlaminar normal stress σ_z will vanish at points located on the edges of the laminate at $y = \pm b$ which is not a correct result. The exact value of σ_z on these edges may, however, be determined by considering the following three-dimensional strain–stress relations (e.g., see Herakovich, 1998):

$$\begin{aligned} \varepsilon_x^{(k)} &= \bar{S}_{11}^{(k)} \sigma_x^{(k)} + \bar{S}_{12}^{(k)} \sigma_y^{(k)} + \bar{S}_{13}^{(k)} \sigma_z^{(k)} + \bar{S}_{16}^{(k)} \sigma_{xy}^{(k)} + \alpha_x^{(k)} \Delta T + \beta_x^{(k)} \Delta M \\ \varepsilon_z^{(k)} &= \bar{S}_{13}^{(k)} \sigma_x^{(k)} + \bar{S}_{23}^{(k)} \sigma_y^{(k)} + \bar{S}_{33}^{(k)} \sigma_z^{(k)} + \bar{S}_{36}^{(k)} \sigma_{xy}^{(k)} + \alpha_z^{(k)} \Delta T + \beta_z^{(k)} \Delta M \end{aligned} \tag{57}$$

where $\bar{S}_{ij}^{(k)}$'s are the off-axis compliances of the kth layer. At the edges of the laminate $u_3^{(k)}$ is specified to vanish (see (47)). Therefore, at all points on these edges (except for points located at the intersections of these edges with interfaces, bottom surface, and top surface of the laminate) it can be concluded:

$$\varepsilon_z \equiv \frac{\partial u_3^{(k)}}{\partial z} = 0 \quad \text{at } y = \pm b. \tag{58}$$

Next, substitution of (47) and (58) (and $\varepsilon_x^{(k)} = B_2$) into (57) results in:

$$B_2 = \bar{S}_{11}^{(k)} \sigma_x^{(k)} + \bar{S}_{13}^{(k)} \sigma_z^{(k)} + \alpha_x^{(k)} \Delta T + \beta_x^{(k)} \Delta M \tag{59a}$$

$$0 = \bar{S}_{13}^{(k)} \sigma_x^{(k)} + \bar{S}_{33}^{(k)} \sigma_z^{(k)} + \alpha_z^{(k)} \Delta T + \beta_z^{(k)} \Delta M. \tag{59b}$$

Upon solving Eqs. (59) the exact value of $\sigma_z^{(k)}$ is obtained to be as follows:

$$\sigma_z^{(k)} = \frac{\bar{S}_{11}^{(k)}(\alpha_z^{(k)}\Delta T + \beta_z^{(k)}\Delta M) + \bar{S}_{13}^{(k)}(B_2 - \alpha_x^{(k)}\Delta T - \beta_x^{(k)}\Delta M)}{\bar{S}_{13}^{(k)^2} - \bar{S}_{11}^{(k)}\bar{S}_{33}^{(k)}}. \tag{60}$$

Relation (60) indicates that the interlaminar normal stress $\sigma_z^{(k)}$ has a constant value at the edges of each lamina (at $y = \pm b$) and, in addition, this constant value changes from one layer to another (adjacent) layer because of changes in fiber orientations.

3. Numerical results and discussions

In this section the validity and accuracy of the theories and procedures introduced here in the present study are first assessed trough several numerical examples by considering cross-ply laminates with special boundary conditions (47) at $y = \pm b$. For this purpose numerical results of ESL and layerwise theories for a uniform temperature change are compared with those of elasticity theory. The interlaminar stresses within various cross-ply, symmetric, and antisymmetric angle-ply laminates with free edges at $y = \pm b$ are then closely examined. The material layers within any laminate are assumed to have identical thickness (h_k), density, and on-axis properties. The mechanical and thermal properties of each lamina are, furthermore, assumed to be the same as those of graphite/epoxy T300/5208 (Herakovich, 1998):

$$\begin{aligned} &E_1 = 132\ \text{GPa}, \quad E_2 = E_3 = 10.8\ \text{GPa}, \quad G_{12} = G_{13} = 5.65\ \text{GPa}, \quad G_{23} = 3.38\ \text{GPa}, \\ &\nu_{12} = \nu_{13} = 0.24, \quad \nu_{23} = 0.59, \quad \alpha_1 = -0.77 \times 10^{-6}/C^\circ, \quad \alpha_2 = \alpha_3 = 0.25 \times 10^{-6}/C^\circ. \end{aligned} \tag{61}$$

Moreover, the thickness of each physical lamina is assumed to be 1 mm (i.e., $h_k = 1$ mm). In addition, since the responses of various laminates due to thermal and hygroscopic loads are similar, only thermal results (due to a uniform temperature change $\Delta T = 1\ ^\circ\text{C}$) are presented here. Furthermore, in the numerical examples the value 5/6 is used for the shear correction factor, k^2, in the first-order plate theories and the interlaminar stress components according to LWT are computed by integrating the local equilibrium equations of elasticity (see, e.g., Reddy, 2003).

Numerical values of B_2 according to FSDT, IFSDT, LWT, and elasticity theory are listed in Table 1 for cross-ply [90°/0°/0°/90°] and [0°/90°/0°/90°] laminates with boundary conditions in (47) under the uniform thermal load $\Delta T = 1\ ^\circ\text{C}$. The ratio of the laminate width to its thickness is assumed to be 5 (i.e., $2b/h = 5$) for the numerical results in Table 1. It is observed that the layerwise theory overestimates the numerical values of B_2 and by, however, increasing the number of numerical layers (p) in each physical layer (see Tahani and Nosier, 2004; Nosier et al., 1993) the results of LWT approach those of the elasticity theory. It is to be noted that the numerical values of B_2 as predicted by FSDT and IFSDT are sufficiently accurate as compared to those of elasticity theory. In addition, the slight differences observed between the first-order theories and the elasticity theory in predicting B_2 have no considerable effects on the interlaminar stress distributions within various laminates. The interlaminar stress components are depicted in Figs. 2 and 3 for thermal problems of cross-ply [90°/0°/0°/90°] and [0°/90°/0°/90°] laminates subjected to the boundary conditions (47) at $y = \pm b$. It

Table 1
Numerical value of the constant parameter $B_2 \times 10^6$ according to FSDT, IFSDT, LWT, and elasticity theory for special boundary conditions in Eqs. (47)

	$P=1$	$P=2$	$P=3$	$P=4$	$P=5$	$P=6$	$P=7$	$P=8$
[90°/0°/0°/90°]								
Layerwise theory	1.7296	1.6980	1.6906	1.6871	1.6852	1.6840	1.6833	1.6828
Elasticity theory	1.6817							
IFSDT	1.7876							
[0°/90°/0°/90°]								
Layerwise theory	1.6633	1.6234	1.6252	1.6113	1.6093	1.6080	1.6072	1.6067
Elasticity theory	1.6051							
FSDT	1.5389							

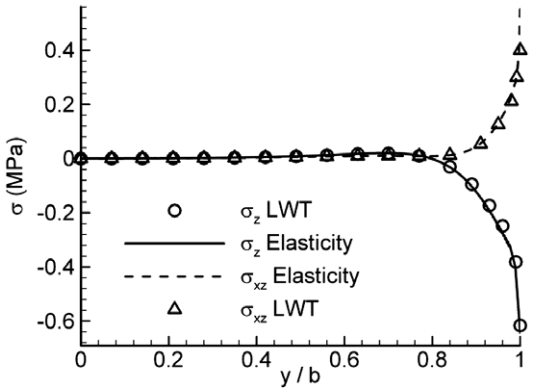

Fig. 2. Distribution of interlaminar stresses near the middle plane of [0°/90°/0°/90°] laminate and in the top 90° layer.

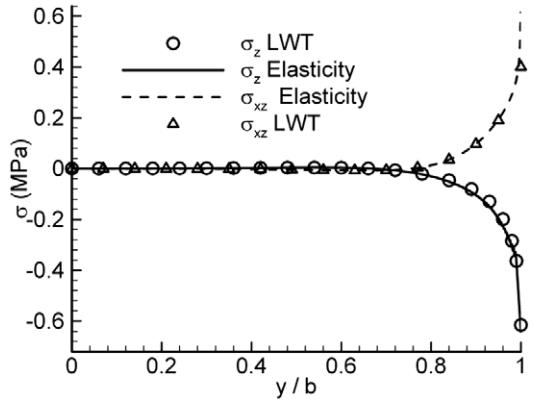

Fig. 3. Distribution of interlaminar stresses near 90°/0° interface of [90°/0°/0°/90°] laminate and in the top 90° layer.

is observed that the results of the layerwise theory are in excellent agreements with those of the elasticity theory.

The free-edge-effect problems are now examined by using several numerical examples. The numerical values of the unknown constant parameters appearing in various displacement fields are presented for cross-ply, symmetric, and antisymmetric angle-ply laminates in Table 2. The results are generated for various width to thickness ratios. Close examination of Table 2 reveals that the FSDT and IFSDT results are sufficiently accurate

Table 2
Unknown constants of displacement field according to FSDT and LWT

Laminate	Theory	Constants	$2b/h = 5$	$2b/h = 10$	$2b/h = 20$
[90°/0°/0°/0°]	FSDT	B_2	7.7625e−7	7.7625e−7	7.7625e−7
		B_6	−1.7317e−3	−1.7317e−3	−1.7317e−3
	LWT	B_2	7.6235e−7	7.7038e−7	7.7697e−7
		B_6	−1.7197e−3	−1.7274e−3	−1.7358e−3
[90°/0°/0°/90°]	IFSDT	B_2	1.5323e−6	1.5472e−6	1.5546e−6
	LWT	B_2	1.5141e−6	1.5386e−6	1.5511e−6
[45°/−10°/−10°/45°]	IFSDT	B_2	−1.8309e−6	−1.9222e−6	−1.9672e−6
	LWT	B_2	−1.7793e−6	−1.8970e−6	−1.9577e−6
[45°/−10°/10°/−45°]	FSDT	B_1	−5.5921e−3	−5.5921e−3	−5.5921e−3
		B_2	−8.6592e−7	−8.6592e−7	−8.6592e−7
	LWT	B_1	−5.5468e−3	−5.5725e−3	−5.5826e−3
		B_2	−7.9602e−7	−8.3327e−7	−8.5260e−7

for thin to moderately thick laminates. For thick laminates, however, numerical investigation indicates that slight inaccuracy in global terms (i.e., terms involving the unknown parameters B_1, B_2, and B_6 appearing in (4)) has insignificant effects on the accuracy of stress distributions within various laminates. It is, therefore, concluded here that the explicit expressions obtained for these parameters according to first-order theories (i.e., relations (30), (31), and (32) for symmetric, cross-ply, and antisymmetric angle-ply laminates) may conveniently be used within other theories such as LWT and elasticity theory (see also Nosier and Bahrami, 2006, 2007). This, in fact, is done here in the remaining of the present study. In order to obtain accurate results for interlaminar stresses, each physical layer is subdivided into, unless otherwise mentioned, 20 numerical layers (i.e., $p = 20$). Moreover, the ratio of width to thickness is assumed to be 10 (i.e., $2b/h = 10$). It is to be noted that for symmetric cross-ply laminates either relation (30) or (31) may be used to determine the single constant parameter B_2 (noting that $B_6 = 0$ for symmetric laminates). Fig. 4 shows the distributions of the interlaminar normal stress σ_z along the two 0°/90° interfaces in the [0°/90°/0°/90°] laminate. It is observed that the σ_z exhibits different behavior at these interfaces. More explicitly, it is seen that the maximum numerical value of σ_z is quite larger in the top 0°/90° interface. The distributions of the interlaminar stresses σ_z and σ_{yz} along the upper and middle interfaces of the symmetric cross-ply [90°/0°/0°/90°] laminate are shown in Fig. 5. Both stresses are seen to grow abruptly in the vicinity of the free edge, while being zero in the interior region of the laminate. It is also noted that the interlaminar shear stress σ_{yz} rises toward the free edge and decreases rather suddenly to zero at the free edge. By increasing the number of numerical layers in each lamina σ_{yz} becomes slightly closer to zero but it may never become zero. This is, most likely, due to the fact that within LWT the generalized stress resultant R_y^k, rather than σ_{yz}, is forced to vanish at the free edge (see Eq. (43)). It is reminded here that

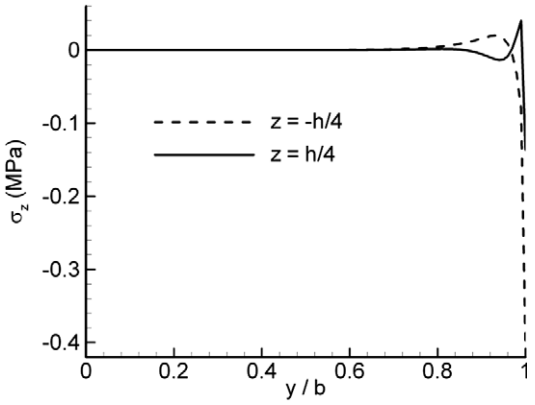

Fig. 4. Interlaminar normal stress along the two 0°/90° interfaces of [0°/90°/0°/90°] laminate.

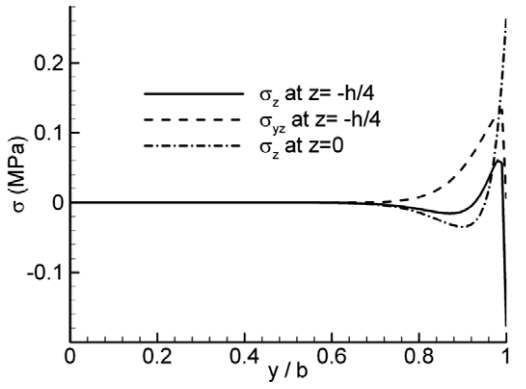

Fig. 5. Distributions of interlaminar stresses along the top and middle interfaces of [90°/0°/0°/90°] laminate.

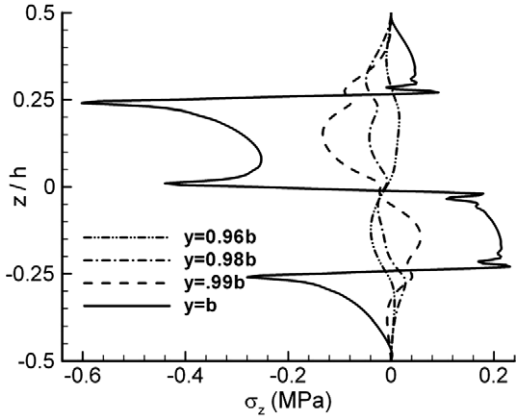

Fig. 6. Interlaminar normal stress σ_z through the thickness of [90°/0°/90°/0°] laminate.

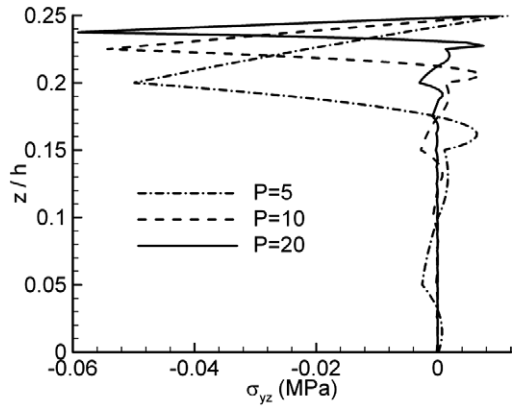

Fig. 7. Distribution of interlaminar shear stress σ_{yz} through the thickness of bottom 90° layer of [0°/90°/90°/0°] laminate.

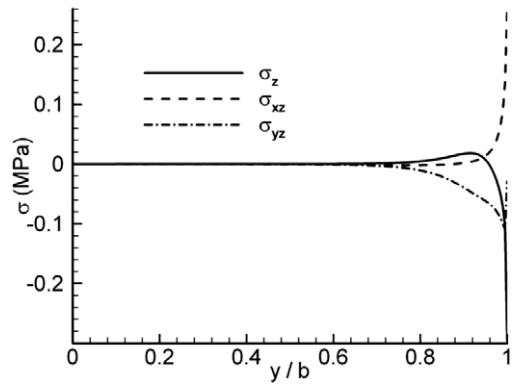

Fig. 8. Distribution of interlaminar stresses along the 25°/−80° interface of [25°/−80°/80°/−25°] laminate.

the interlaminar shear stress σ_{xz} is identically zero everywhere in cross-ply laminates. Also, due to symmetry, the interlaminar shear stress σ_{yz} vanishes at the middle surface of symmetric cross-ply laminates. The variations of interlaminar normal stress σ_z through the thickness of the unsymmetric cross-ply laminate [90°/0°/90°/0°] are depicted in Fig. 6 as the free edge is approached. It is observed that the maximum negative value of σ_z occurs within the top 0° layer and the maximum positive value of σ_z occurs within the bottom 90° layer

both near the 90°/0° interfaces at the free edge (i.e., $y = b$). It is also seen that σ_z diminishes away from the free edge as the interior region of the laminate is approached. Fig. 7 shows the variations of transverse shear stress σ_{yz} at the free edge (i.e., $y = b$) and through the thickness of the bottom 90° layer of the [0°/90°/90°/0°] laminate. It is clear from the figure that σ_{yz} has a nonzero value at the interface-edge junction (i.e., interface corner) of the laminate. A close examination of Fig. 7 reveals that, except for the interface corner point, the value of σ_{yz} along the free edge of the laminate approaches zero as the number of numerical layers in each physical ply, p, is increased. The variations of the interlaminar normal and shear stresses along the upper interface (i.e., the 25°/−80° interface) of the antisymmetric angle-ply laminate [25°/−80°/80°/−25°] are plotted in Fig. 8. It is seen that the magnitude of σ_{yz} is quite smaller than those of σ_z and σ_{xz} (with σ_{xz} and σ_z surprisingly having similar magnitudes). It is reminded here that extensive numerical studies indicate that the interlaminar shear stress σ_{yz} is equal to zero at the middle surface of all antisymmetric angle-ply laminates subjected to uniform hygrothermal loads. The distributions of interlaminar stresses σ_z and σ_{xz} across the 0°/60° interfaces of [−60°/0°/0°/60°] and [0°/60°/−60°/0°] laminates are compared in Fig. 9a and b. It is observed that both transverse normal stress σ_z and transverse shear stress σ_{xz} exhibit similar behavior in the two laminates. The maximum interfacial values for both σ_z and σ_{xz} occur, however, in the [0°/60°/−60°/0°] laminate. The distributions of through-the-thickness interlaminar normal stress σ_z at $y = b$ for the antisymmetric angle-ply laminate [45°/60°/−60°/−45°] and the symmetric laminate [45°/60°/60°/45°] are shown in Fig. 10. It is observed that the value of σ_z at the free edge is noticeably larger in the antisymmetric angle-ply laminate. The maximum value of σ_z in the [45°/60°/−60°/−45°] laminate occurs at the middle surface while the maximum value of σ_z in [45°/60°/60°/45°] occurs in the 60° layers near the top and bottom interfaces. It is to be noted that, in both symmetric and antisymmetric angle-ply laminates, the interlaminar normal stress σ_z is an even function of thickness coordinate. Similarly, the variations of interlaminar shear stress σ_{xz} through the thickness and at the free edge of the $[(45°/-45°)_2]$ and $[45°/-45°]_s$ laminates are presented in Fig. 11. It is noticed from this figure that

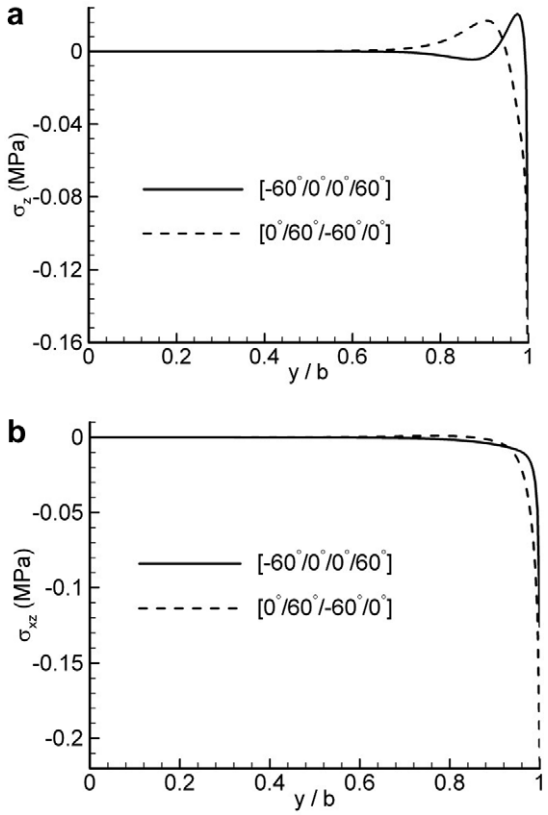

Fig. 9. (a) Interlaminar normal stress σ_z along the 0°/60° interfaces of [−60°/0°/0°/60°] and [0°/60°/60°/0°] laminates. (b) Interlaminar shear stress σ_{xz} along the 0°/60° interfaces of [−60°/0°/0°/60°] and [0°/60°/60°/0°] laminates.

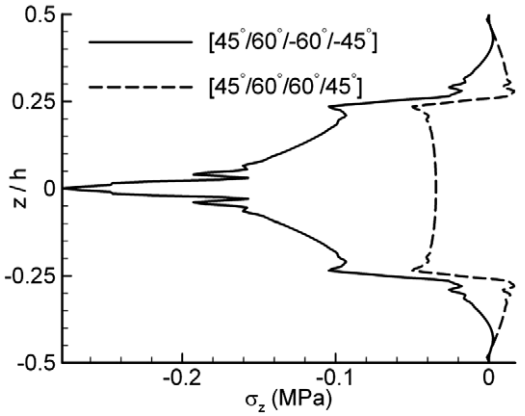

Fig. 10. Distributions of interlaminar normal stress σ_z through the thickness of [45°/60°/−60°/−45°] and [45°/60°/60°/45°] laminates.

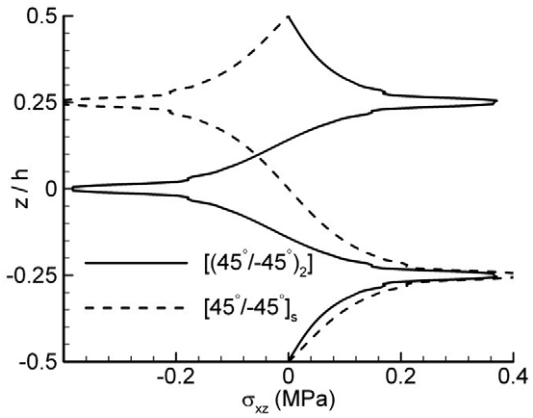

Fig. 11. Distributions of interlaminar shear stress σ_{xz} through the thickness of $[(45°/-45°)_2]$ and $[45°/-45°]_s$ laminates.

in the antisymmetric angle-ply laminate the maximum positive values of σ_{xz} occur near the 45°/−45° interfaces whereas the maximum negative value of σ_{xz} occurs at the middle surface of the laminate. In the symmetric laminate, however, the maximum positive and negative values of σ_{xz} occur near the −45°/45° and 45°/−45° interfaces, respectively. It is significant to note that the magnitudes of maximum values of σ_{xz} for both laminates are approximately equal, with σ_{xz} being an odd (even) function of thickness coordinate in symmetric (antisymmetric angle-ply) laminates.

Finally, the effect of fiber orientation is examined in Fig. 12a and b by comparing the variations of interlaminar normal stress σ_z at the top interface-edge and middle surface-edge junctions of the [0°/θ/θ/0°] and [0°/θ/−θ/0°] laminates as a function of θ. It is observed that at the top interface-edge (i.e., 0°/θ interface-edge) junctions the two laminates display very similar behavior, with the numerical values of σ_z being approximately identical. At the middle surface-edge junction, however, the distributions of σ_z in the two laminates are, except for small θ's, quite different. The maximum values of σ_z at the top interface-edge junction occur at $\theta = 90°$ in both laminates whereas at the middle surface-edge junction σ_z becomes maximum when $\theta \approx 55°$ in the antisymmetric angle-ply laminate and when $\theta = 90°$ in the symmetric laminate.

4. Conclusions

In the present investigation an elasticity formulation is presented for the displacement field of a long generally stacked laminate subjected to hygrothermal loads. It is found that the components of the displacements

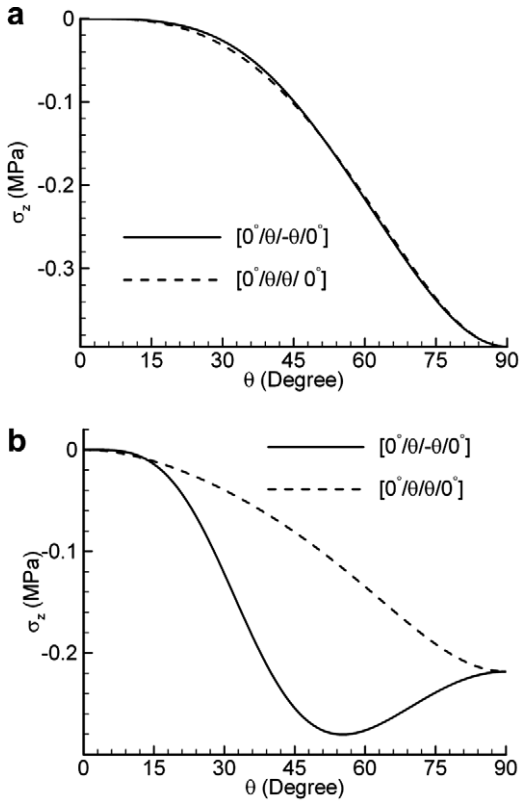

Fig. 12. (a) Interlaminar normal stress σ_z at the top interface-edge junctions (i.e., $0°/\theta$ interface-edge junctions) of the $[0°/\theta/\theta/0°]$ and $[0°/\theta/-\theta/0°]$ laminates as a function of θ. (b) Interlaminar normal stress σ_z at the middle interface-edge junctions of the $[0°/\theta/\theta/0°]$ and $[0°/\theta/-\theta/0°]$ laminates as a function of θ.

field are composed of two distinct parts, signifying the global and local deformations within laminates. Based on physical arguments regarding the behavior of symmetric, cross-ply, and antisymmetric angle-ply laminates special displacement fields are obtained for such laminates. The ESL theories are then employed to determine the unknown constant parameters appearing in the global deformation part of various displacement fields. It is also found that for each lamination scheme an appropriate ESL theory must be employed for the efficient and accurate prediction of these parameters. For cross-ply and antisymmetric angle-ply laminates it is found that the usual first-order theory (Mindlin–Reissner plate theory) yields accurate results for the unknown constant parameters appearing in various displacement fields. Numerical investigations, however, reveal that for symmetric laminates the usual first-order theory (FSDT) is inadequate in predicting these parameters. Therefore, an improved first-order theory (IFSDT) is introduced to obtain these parameters for symmetric laminates. Next, Reddy's layerwise theory (LWT) is utilized to calculate the interlaminar stresses. The unknown constants appearing in various displacement fields are also determined within LWT. For special boundary and loading conditions an analytical elasticity solution is presented to verify the accuracy of LWT, in predicting the interlaminar stresses and B_2, and that of FSDT and IFSDT in predicting B_2. Excellent agreements are seen to exist between the results of LWT and the elasticity theory. Several numerical results according to LWT are then developed for the free-edge interlaminar stresses through the thickness and across the interfaces of various cross-ply, symmetric, and antisymmetric angle-ply laminates.

Appendix A

The coefficients $\bar{D}_{22}$, $\bar{D}_{26}$, and $\bar{D}_{66}$ appearing in (26) are given as follows:

$$\bar{D}_{22} = D_{22} + \frac{\tilde{B}_{26}(A_{26}\tilde{B}_{22} - A_{22}\tilde{B}_{26}) + \tilde{B}_{22}(A_{26}\tilde{B}_{26} - A_{66}\tilde{B}_{22})}{A_{22}A_{66} - A_{26}^2}$$

$$\bar{D}_{26} = D_{26} + \frac{\tilde{B}_{26}(A_{26}\tilde{B}_{26} - A_{22}\tilde{B}_{66}) + \tilde{B}_{22}(A_{26}\tilde{B}_{66} - A_{66}\tilde{B}_{26})}{A_{22}A_{66} - A_{26}^2}$$

$$\bar{D}_{66} = D_{66} + \frac{\tilde{B}_{66}(A_{26}\tilde{B}_{26} - A_{22}\tilde{B}_{66}) + \tilde{B}_{26}(A_{26}\tilde{B}_{66} - A_{66}\tilde{B}_{26})}{A_{22}A_{66} - A_{26}^2}.$$

The constant parameters in Eqs. (28a) and (28b) are defined as:

$$(d_1, d_2) = \frac{1}{a_1a_4 - a_2a_3}(a_2\bar{B}_{16} - a_4\bar{B}_{12}, a_3\bar{B}_{12} - a_1\bar{B}_{16})$$
$$(m_y^{\mathrm{T}}, m_{xy}^{\mathrm{T}}) = \frac{1}{a_1a_4 - a_2a_3}(a_4\bar{M}_y^{\mathrm{T}} - a_2\bar{M}_{xy}^{\mathrm{T}}, a_1\bar{M}_{xy}^{\mathrm{T}} - a_3\bar{M}_y^{\mathrm{T}})$$
$$(m_y^{\mathrm{H}}, m_{xy}^{\mathrm{H}}) = \frac{1}{a_1a_4 - a_2a_3}(a_4\bar{M}_y^{\mathrm{H}} - a_2\bar{M}_{xy}^{\mathrm{H}}, a_1\bar{M}_{xy}^{\mathrm{H}} - a_3\bar{M}_y^{\mathrm{H}})$$

where

$$a_1 = (\bar{D}_{26} + \bar{D}_1\bar{D}_{22})\lambda_1\cosh(\lambda_1 b), \quad a_2 = (\bar{D}_{26} + \bar{D}_2\bar{D}_{22})\lambda_2\cosh(\lambda_2 b)$$
$$a_3 = (\bar{D}_{66} + \bar{D}_1\bar{D}_{26})\lambda_1\cosh(\lambda_1 b), \quad a_4 = (\bar{D}_{66} + \bar{D}_2\bar{D}_{26})\lambda_2\cosh(\lambda_2 b)$$

$$\bar{B}_{12} = \tilde{B}_{12} + \frac{\tilde{B}_{26}(A_{12}A_{26} - A_{16}A_{22}) + \tilde{B}_{22}(A_{16}A_{26} - A_{12}A_{66})}{A_{22}A_{66} - A_{26}^2}$$

$$\bar{B}_{16} = \tilde{B}_{16} + \frac{\tilde{B}_{66}(A_{12}A_{26} - A_{16}A_{22}) + \tilde{B}_{26}(A_{16}A_{26} - A_{12}A_{66})}{A_{22}A_{66} - A_{26}^2}$$

and

$$\bar{M}_y^{\mathrm{T}} = \tilde{M}_y^{\mathrm{T}} - \frac{\tilde{B}_{26}(A_{22}N_{xy}^{\mathrm{T}} - A_{26}N_y^{\mathrm{T}}) + \tilde{B}_{22}(A_{66}N_y^{\mathrm{T}} - A_{26}N_{xy}^{\mathrm{T}})}{A_{22}A_{66} - A_{26}^2}$$

$$\bar{M}_{xy}^{\mathrm{T}} = \tilde{M}_{xy}^{\mathrm{T}} - \frac{\tilde{B}_{66}(A_{22}N_{xy}^{\mathrm{T}} - A_{26}N_y^{\mathrm{T}}) + \tilde{B}_{26}(A_{66}N_y^{\mathrm{T}} - A_{26}N_{xy}^{\mathrm{T}})}{A_{22}A_{66} - A_{26}^2}$$

$$\bar{M}_y^{\mathrm{H}} = \tilde{M}_y^{\mathrm{H}} - \frac{\tilde{B}_{26}(A_{22}N_{xy}^{\mathrm{H}} - A_{26}N_y^{\mathrm{H}}) + \tilde{B}_{22}(A_{66}N_y^{\mathrm{H}} - A_{26}N_{xy}^{\mathrm{H}})}{A_{22}A_{66} - A_{26}^2}$$

$$\bar{M}_{xy}^{\mathrm{H}} = \tilde{M}_{xy}^{\mathrm{H}} - \frac{\tilde{B}_{66}(A_{22}N_{xy}^{\mathrm{H}} - A_{26}N_y^{\mathrm{H}}) + \tilde{B}_{26}(A_{66}N_y^{\mathrm{H}} - A_{26}N_{xy}^{\mathrm{H}})}{A_{22}A_{66} - A_{26}^2}.$$

In addition, the constant coefficients appearing in (30) are defined as follows:

$$\hat{h} = \bar{A}_{11}b + d_1(\bar{B}_{16} + \bar{B}_{12}\bar{D}_1)\sinh(\lambda_1 b) + d_2(\bar{B}_{16} + \bar{B}_{12}\bar{D}_2)\sinh(\lambda_2 b)$$
$$n_x^{\mathrm{T}} = b\bar{N}_x^{\mathrm{T}} - m_y^{\mathrm{T}}(\bar{B}_{16} + \bar{B}_{12}\bar{D}_1)\sinh(\lambda_1 b) - m_{xy}^{\mathrm{T}}(\bar{B}_{16} + \bar{B}_{12}\bar{D}_2)\sinh(\lambda_2 b)$$
$$n_x^{\mathrm{H}} = b\bar{N}_x^{\mathrm{H}} - m_y^{\mathrm{H}}(\bar{B}_{16} + \bar{B}_{12}\bar{D}_1)\sinh(\lambda_1 b) - m_{xy}^{\mathrm{H}}(\bar{B}_{16} + \bar{B}_{12}\bar{D}_2)\sinh(\lambda_2 b)$$

where

$$\bar{A}_{11} = A_{11} + \frac{A_{16}(A_{12}A_{26} - A_{16}A_{22}) + A_{12}(A_{16}A_{26} - A_{12}A_{66})}{A_{22}A_{66} - A_{26}^2}$$

and

$$\bar{N}_x^{\mathrm{T}} = N_x^{\mathrm{T}} - \frac{A_{16}(A_{22}N_{xy}^{\mathrm{T}} - A_{26}N_y^{\mathrm{T}}) + A_{12}(A_{66}N_y^{\mathrm{T}} - A_{26}N_{xy}^{\mathrm{T}})}{A_{22}A_{66} - A_{26}^2}$$

$$\bar{N}_x^{\mathrm{H}} = N_x^{\mathrm{H}} - \frac{A_{16}(A_{22}N_{xy}^{\mathrm{H}} - A_{26}N_y^{\mathrm{H}}) + A_{12}(A_{66}N_y^{\mathrm{H}} - A_{26}N_{xy}^{\mathrm{H}})}{A_{22}A_{66} - A_{26}^2}.$$

Appendix B

The constant coefficients appearing in (31) are given as follows:

$$h_1 = A_{11}a_1 + A_{12}a_2 + B_{12}a_3, \quad h_2 = B_{11}a_1 + A_{12}a_4 + B_{12}a_5$$
$$h_3 = B_{11}a_1 + B_{12}a_2 + D_{12}a_3, \quad h_4 = D_{11}a_1 + B_{12}a_4 + D_{12}a_5$$

and

$$n_x^{\mathrm{T}} = N_x^{\mathrm{T}}a_1 + N_y^{\mathrm{T}}a_2 + M_y^{\mathrm{T}}a_3, \quad m_x^{\mathrm{T}} = M_x^{\mathrm{T}}a_1 + N_y^{\mathrm{T}}a_4 + M_y^{\mathrm{T}}a_5$$
$$n_x^{\mathrm{H}} = N_x^{\mathrm{H}}a_1 + N_y^{\mathrm{H}}a_2 + M_y^{\mathrm{H}}a_3, \quad m_x^{\mathrm{H}} = M_x^{\mathrm{H}}a_1 + N_y^{\mathrm{H}}a_4 + M_y^{\mathrm{H}}a_5$$

where

$$a_1 = A_{22}D_{22} - B_{22}^2, \quad a_2 = B_{12}B_{22} - A_{12}D_{22}, \quad a_3 = A_{12}B_{22} - A_{22}B_{12}$$
$$a_4 = B_{22}D_{12} - B_{12}D_{22}, \quad a_5 = B_{12}B_{22} - A_{22}D_{12}.$$

It is reminded here that the laminate rigidities and stress, thermal, and hygroscopic resultants are the same as those defined in Eqs. (19), (21), (22), and (23). Furthermore, here:

$$(M_x^{\mathrm{T}}, M_y^{\mathrm{T}}) = \int_{-h/2}^{h/2} [(\bar{Q}_{11}, \bar{Q}_{12})\alpha_x + (\bar{Q}_{12}, \bar{Q}_{22})\alpha_y]\Delta T z \, \mathrm{d}z$$

$$(M_x^{\mathrm{H}}, M_y^{\mathrm{H}}) = \int_{-h/2}^{h/2} [(\bar{Q}_{11}, \bar{Q}_{12})\beta_x + (\bar{Q}_{12}, \bar{Q}_{22})\beta_y]\Delta M z \, \mathrm{d}z$$

and

$$B_{ij} = \int_{-h/2}^{h/2} \bar{Q}_{ij} z \, \mathrm{d}z.$$

It is observed that the constant parameters B_2 and B_6 appearing in (31) are independent of shear correction factor. In other words, the results presented in (31) for B_2 and B_6 are also obtainable from the classical lamination theory.

Appendix C

The constant coefficients appearing in (32) are given by:

$$h_1 = 2(A_{12}B_{26} - A_{22}B_{16})$$
$$h_2 = A_{11}A_{22} - A_{12}^2$$
$$h_3 = 2(B_{26}^2 - A_{22}D_{66})$$
$$h_4 = A_{22}B_{16} - A_{12}B_{26}$$

and

$$
\begin{aligned}
n_x^{\mathrm{T}} &= A_{22}N_x^{\mathrm{T}} - A_{12}N_y^{\mathrm{T}}\\
m_{xy}^{\mathrm{T}} &= A_{22}M_{xy}^{\mathrm{T}} - B_{26}N_y^{\mathrm{T}}\\
n_x^{\mathrm{H}} &= A_{22}N_x^{\mathrm{H}} - A_{12}N_y^{\mathrm{H}}\\
m_{xy}^{\mathrm{H}} &= A_{22}M_{xy}^{\mathrm{H}} - B_{26}N_y^{\mathrm{H}}
\end{aligned}
$$

where

$$
\begin{aligned}
M_{xy}^{\mathrm{T}} &= \int_{-h/2}^{h/2}[\bar{Q}_{16}\alpha_x + \bar{Q}_{26}\alpha_y + \bar{Q}_{66}\alpha_{xy}]\Delta T z\,\mathrm{d}z\\
M_{xy}^{\mathrm{H}} &= \int_{-h/2}^{h/2}[\bar{Q}_{16}\beta_x + \bar{Q}_{26}\beta_y + \bar{Q}_{66}\beta_{xy}]\Delta M z\,\mathrm{d}z
\end{aligned}
$$

with the remaining thermal and hygroscopic resultants being the same as those defined in (22a) and (23a). For antisymmetric angle-ply laminates the results in (32) may also be arrived at by using the classical lamination theory.

Appendix D

The laminate rigidities, introduced in (40), are given as follows (also see Nosier and Bahrami, 2006, 2007):

$$
(A_{pq}^{kj}, B_{pq}^{kj}, D_{pq}^{kj}) = \begin{cases}
\left(-\frac{\bar{C}_{pq}^{(k-1)}}{h_{k-1}}, -\frac{\bar{C}_{pq}^{(k-1)}}{2}, \frac{h_{k-1}\bar{C}_{pq}^{(k-1)}}{6}\right) & \text{if } j = k-1\\
\left(\frac{\bar{C}_{pq}^{(k-1)}}{h_{k-1}} + \frac{\bar{C}_{pq}^{(k)}}{h_k}, \frac{\bar{C}_{pq}^{(k-1)}}{2} - \frac{\bar{C}_{pq}^{(k)}}{2}, \frac{h_{k-1}\bar{C}_{pq}^{(k-1)}}{3} + \frac{h_k\bar{C}_{pq}^{(k)}}{3}\right) & \text{if } j = k\\
\left(-\frac{\bar{C}_{pq}^{(k)}}{h_k}, \frac{\bar{C}_{pq}^{(k)}}{2}, \frac{h_k\bar{C}_{pq}^{(k)}}{6}\right) & \text{if } j = k+1\\
(0,0,0) & \text{if } j < k-1 \text{ or } j > k+1
\end{cases}
$$

and

$$
(A_{pq}^{k}, B_{pq}^{k}, \bar{B}_{pq}^{k}, D_{pq}^{k}) = \begin{cases}
\left(-\bar{C}_{pq}^{(1)}, \frac{h_1\bar{C}_{pq}^{(1)}}{2}, \bar{C}_{pq}^{(1)}\frac{z_1^2-z_2^2}{2h_1}, \frac{\bar{C}_{pq}^{(1)}}{h_1}\left[\frac{z_1^3-z_2^3}{3} - z_2\frac{z_1^2-z_2^2}{2}\right]\right) & \text{if } k = 1\\
\left(\bar{C}_{pq}^{(k-1)}, \frac{h_{k-1}\bar{C}_{pq}^{(k-1)}}{2}, \bar{C}_{pq}^{(k-1)}\frac{z_k^2-z_{k-1}^2}{2h_{k-1}}, \frac{\bar{C}_{pq}^{(k-1)}}{h_{k-1}}\left[\frac{z_k^3-z_{k-1}^3}{3} - z_{k-1}\frac{z_k^2-z_{k-1}^2}{2}\right]\right) & \text{if } k = N+1\\
\left(\bar{C}_{pq}^{(k-1)} - \bar{C}_{pq}^{(k)}, \frac{h_{k-1}\bar{C}_{pq}^{(k-1)}}{2} + \frac{h_k\bar{C}_{pq}^{(k)}}{2}, \bar{C}_{pq}^{(k-1)}\frac{z_k^2-z_{k-1}^2}{2h_{k-1}} + \bar{C}_{pq}^{(k)}\frac{z_k^2-z_{k+1}^2}{2h_k},\right.\\
\left.\frac{\bar{C}_{pq}^{(k-1)}}{h_{k-1}}\left[\frac{z_k^3-z_{k-1}^3}{3} - z_{k-1}\frac{z_k^2-z_{k-1}^2}{2}\right] + \frac{\bar{C}_{pq}^{(k)}}{h_k}\left[\frac{z_k^3-z_{k+1}^3}{3} - z_{k+1}\frac{z_k^2-z_{k+1}^2}{2}\right]\right) & \text{if } 1 < k < N+1.
\end{cases}
$$

References

Cho, M., Kim, H.S., 2000. Iterative free-edge stress analysis of composite laminates under extension, bending, twisting and thermal loadings. International Journal of Solids and Structures 37 (3), 435–459.

Fung, Y.C., Tong, P., 2001. Classical and Computational Solid Mechanics. World Scientific, New Jersey.

Herakovich, C.T., 1998. Mechanics of Fibrous Composites. John Wiley & Sons, New York.

Jones, R.M., 1998. Mechanics of Composite Materials. Taylor & francis, London.

Kant, T., Swaminathan, K., 2000. Estimation of transverse/interlaminar stresses in laminated composites-a selective review and survey of current developments. Composite Structures 49, 65–75.

Kassapoglou, C., Lagace, P.A., 1986. An efficient method for the calculation of interlaminar stresses in composite materials. Journal of Applied Mechanics 53, 744–750.

Kassapoglou, C., Lagace, P.A., 1987. Closed form solutions for the interlaminar stress field in angle-ply and cross-ply laminates. Journal of Composite Materials 21 (1), 292–308.

Kim, T., Atlury, S.N., 1995. Analysis of edge stresses in composite laminates under combined thermo-mechanical loading using a complementary energy approach. Computational Mechanics 16, 83–87.

Lekhnitskii, S.G., 1981. Theory of Elasticity of an Anisotropic Body. Mir Publishers.

Matsunaga, H., 2004. A Comparison between 2-D single-layer and 3-D layerwise theories for computing interlaminar stresses of laminated composite and sandwich plates subjected to thermal loadings. Composite Structures 64, 161–177.

Morton, S.K., Webber, J.P.H., 1993. Interlaminar failure due to mechanical and thermal stresses at the free edges of laminated plates. Composite Science and Technology 47, 1–13.

Nosier, A., Bahrami, A., 2006. Free-edge stresses in antisymmetric angle-ply laminates in extension and torsion. International Journal of Solids and Structures 43, 6800–6816.

Nosier, A., Bahrami, A., 2007. Interlaminar stresses in antisymmetric angle-ply laminates. Composite Structures 78, 18–33.

Nosier, A., Kapania, R.K., Reddy, J.N., 1993. Free vibration analysis of laminated plates using a layerwise theory. AIAA Journal 13 (12), 2335–2346.

Pagano, N.J., 1974. On the calculation of interlaminar normal stress in composite laminate. Journal of Composite Materials 8, 65–81.

Pipes, R.B., Pagano, N.J., 1970. Interlaminar stresses in composite laminates under uniform axial extension. Journal of Composite Materials 4, 538–548.

Reddy, J.N., 2003. Mechanics of Laminated Composite Plates and Shells: Theory and Analysis. CRC Press, New York.

Rohwer, K., Rolfes, R., Sparr, H., 2001. Higher-order theories for thermal stresses in layered plates. International Journal of Solids and Structures 38, 3673–3687.

Tahani, M., Nosier, A., 2003. Free edge stress analysis of general cross-ply composite laminates under extension and thermal loading. Composite Structures 60, 91–103.

Tahani, M., Nosier, A., 2004. Accurate determination of interlaminar stresses in general cross-ply laminates. Mechanics of Advanced Materials and Structures 11 (1), 67–92.

Wang, A.S.D., Crossman, F.W., 1977a. Some new results on edge effect in symmetric composite laminates. Journal of Composite Materials 11, 92–106.

Wang, A.S.D., Crossman, F.W., 1977b. Edge effects on thermally induced stresses in composite laminates. Journal of Composite Materials 11, 300–312.

Wang, S.S., Choi, I., 1982. Boundary-layer hygroscopic stresses in angle-ply composite laminates. AIAA Journal 20 (11), 1592–1598.

Wang, Y.R., Chou, T.W., 1989. Three-dimensional transient interlaminar stresses in angle-ply composites. Journal of Applied Mechanics 56, 601–608.

Webber, J.P.H., Morton, S.K., 1993. An analytical solution for the thermal stresses at the free edges of laminated plates. Composite Science and Technology 46, 175–185.

Yin, W.L., 1997. The effect of temperature gradient on the free-edge interlaminar stresses in multilayered structures. Journal of Composite Materials 31 (24), 2460–2477.